Stratigraphy and chronology of Upper Cretaceous–lower Paleogene strata in Bolivia and northwest Argentina

T. Sempere — *Département T.O.A., Orstom, 213 rue Lafayette, 75010 Paris, France*

R. F. Butler*, D. R. Richards — *Department of Geosciences, University of Arizona, Tucson, Arizona 85721*

L. G. Marshall — *Institute of Human Origins, 1288 9th Street, Berkeley, California 94710*

W. Sharp, C. C. Swisher III — *Berkeley Geochronology Center, 2455 Ridge Road, Berkeley, California 94709*

ABSTRACT

Integration of sequence stratigraphy, magnetostratigraphy, Ar/Ar dating, and paleontology considerably advances knowledge of the Late Cretaceous–early Paleogene chronostratigraphy and tectonic evolution of Bolivia and adjacent areas. The partly restricted marine El Molino Formation spans the Maastrichtian and Danian (~73–60.0 Ma). Deposition of the alluvial to lacustrine Santa Lucía Formation occurred between 60.0 and 58.2 Ma. The widespread erosional unconformity at the base of the Cayara Formation is 58.2 Ma. This unconformity separates the Upper Puca and Corocoro supersequences in Bolivia, and is thus coeval with the Zuni-Tejas sequence boundary of North America. The thick overlying Potoco and Camargo formations represent a late Paleocene–Oligocene foreland fill.

The onset of shortening along the Pacific margin at ~89 Ma initially produced rifting in the distal foreland. Santonian–Campanian eastward-onlapping deposits indicate subsequent waning of tectonic activity along the margin. Significant tectonism and magmatism resumed along the margin at ~73 Ma and produced an abrupt increase in subsidence rate and other related phenomena in the basin. Subsidence was maximum between ~71 and ~66 Ma. Due to the early Maastrichtian global sea-level high, marine waters ingressed from the northwest into this underfilled basin. Subsidence decreased during the Late Maastrichtian and was low during the Danian. It increased again in the latest Danian, for which a slight transgression is recorded, and peaked in the early Selandian. Tectonism between 59.5 and 58.2 Ma produced a variety of deformational and sedimentary effects in the basin and correlates with the end of emplacement of the Coastal batholith. The subsequent 58.2 Ma major unconformity marks the onset of continental foreland basin development, which extended into Andean Bolivia during the late Paleocene–Oligocene interval. This basin underwent internal deformation as early as Eocene time in the Altiplano and Cordillera Oriental. These early structures, previously assigned to the late Oligocene–early Miocene orogeny, probably accommodated observed tectonic rotations in the Eocene–Oligocene.

*Corresponding author; E-mail: butler@pmag.geo.arizona.edu

INTRODUCTION

The Andean basin of South America was an underfilled foreland basin of the early Andes in the Late Cretaceous and Paleogene. Periodic marine connections with the Caribbean region occurred in the Maastrichtian–Danian (Fig. 1). Due to considerable eastward propagation of deformation since the late Oligocene, Bolivia has excellent exposures of Cretaceous and Cenozoic strata, including rocks suitable for paleomagnetic studies and Ar/Ar dating.

We summarize and update the Late Cretaceous–early Paleogene stratigraphy of Bolivia and adjacent areas. In particular we provide a detailed chronostratigraphy of the Maastrichtian and Paleocene strata of the central Andean basin that integrates magnetostratigraphy, Ar/Ar dating, sequence stratigraphy, and paleontology. Our magnetostratigraphic study is the first for the Maastrichtian and the second for the Paleocene in South Ameri~It encompasses ~17 m.y. and is the most complete, to date, for this continent. The results allow the position of the Cretaceous-Tertiary (K-T) boundary to be constrained within ~43 m in our reference section and provide geochronologic calibration of fossiliferous strata across the boundary.

Although knowledge of the stratigraphy, basin geometry, and deformation has improved in the past 10 yr, early Andean tectonic history remains imprecise. Our chronostratigraphy of the Late Cretaceous–early Paleogene infilling of the paleo-Andean foreland basin provides a refined chronology of the early tectonic evolution of the basin. We demonstrate that the major tectonic event that initiated development of the late Paleocene–Oligocene foreland basin occurred between 59.5 and 58.2 Ma, and correlate this initiation with tectonic events in the Pacific and North America.

GEOLOGIC CONTEXT

Knowledge of the Phanerozoic evolution of the central Andean region was summarized by Sempere (1995). Subsidence in the Andean basin was initiated in the early Paleozoic and reactivated at various times during the Phanerozoic in response to the tectonic evolution along the western margin of South Ameri~During most of Silurian to Paleogene time, Bolivia was located at the southern tip of a longitudinal subsident domain that was parallel to the Pacific margin of South America and generally deepened toward the north or northwest along its axis (Fig. 1). Throughout this time, this domain remained bounded to the south by the Sierras Pampeanas massif in

Data Repository item 9719 contains additional material related to this article.

GSA Bulletin; June 1997; v. 109; no. 6; p. 709–727; 14 figures; 1 table.

northwest Argentina. An important consequence of this geometry is that, at least from Silurian to Danian time, marine waters transgressed into Bolivia from the north or northwest.

The Potosí basin of Andean Bolivia, which had endorheic infilling during the Late Jurassic–Early Cretaceous, became the southern portion of the central Andean back-arc basin in mid-Cretaceous time (Sempere, 1994). The Potosí basin evolved as the distal part of the wide, underfilled foreland basin of the emerging Andes in Senonian–middle Paleocene time, and as their continental, external foreland basin during the late Paleocene–early Oligocene. Some western areas of the Potosí basin underwent locally significant deformation as early as Eocene time, while foreland sedimentation continued. Eastward propagation of Andean deformation increased considerably after the late Oligocene (Sempere et al., 1990).

A number of tectonostratigraphic domains were displaced and shortened, sometimes considerably, during the Andean orogeny (Sempere, 1995). Neighboring points separated by boundary faults between domains (Fig. 1) were usually more distant at the time of their pre-Neogene sedimentation. The pronounced Andean shortening explains why facies, thicknesses, and other characteristics of many rock units sometimes change substantially over what are now short distances. For this reason, the boundaries of the main tectonostratigraphic domains distinguished in Bolivia are illustrated on the paleogeographic maps of this paper, although they were generally not active at the time of deposition.

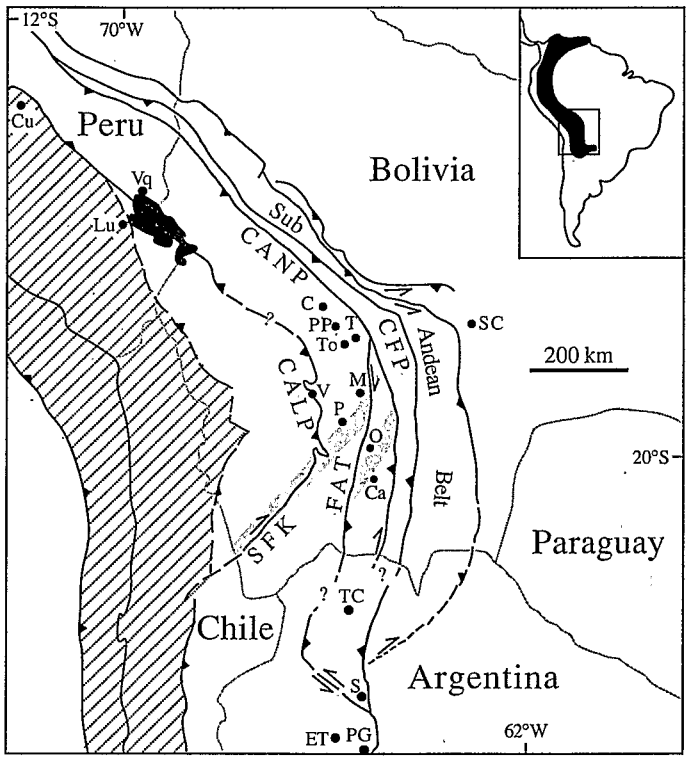

Figure 1. Neogene structural sketch map of the central Andes (simplified after Sempere, 1995) and localities mentioned in text. C—Cochabamba, Ca—Camargo, Ch—Chita, Cu—Cuzco, M—Maragua, O—Otavi, P—Potosí, PG—Pampa Grande, PP—Pajcha Pata, S—Salta, SC—Santa Cruz, T—Tiupampa, To—Torotoro, V—Vilcapujio, Vq—Vilquechico. Hatched—western Andean belt; Spanish abbreviations for faults: CALP—Cabalgamiento Altiplánico Principal; CANP—Main Andean thrust; CFP—Main Frontal thrust; FAT—Aiquile-Tupiza fault; SFK—Khenayani fault system; wide stippled line—Khenayani-Turuchipa paleostructural corridor. Fine stippled lines are political borders. Inset: Late Cretaceous Andean basin (black) and location of map (box) within South America.

The southern half of Andean Bolivia is crossed by a northeast-striking major tectonic element, the Khenayani-Turuchipa paleostructural corridor (CPKT in Fig. 1), which appears to have influenced Phanerozoic sedimentation and deformation in southwestern Bolivia (Sempere et al., 1991). Thicknesses of Cretaceous–Paleocene units are notably greater northwest of the Khenayani-Turuchipa paleostructural corridor (Sempere, 1994).

LITHOSTRATIGRAPHY

The stratigraphic units discussed in this paper (Fig. 2) belong to the Upper Puca supersequence (Senonian–late Paleocene) and to the lower half of the Corocoro supersequence (late Paleocene–Holocene) (see Sempere, 1990, 1995). Most of these units were defined by Lohmann and Branisa (1962) in the Potosí region. Marginal areas, such as the Cochabamba region and Camargo syncline, contain facies and stratigraphic units somewhat different from the Potosí region. Age determinations were discussed by Jaillard and Sempere (1989, 1991), Sempere (1990, 1994), Gayet et al. (1991), and are discussed in this paper. Regional correlations are shown in Figure 3 and are discussed below. The stratigraphy, paleogeography, and tectonic context of this mainly continental Senonian–Oligocene succession indicates deposition in the axial to distal part of the Andean underfilled foreland basin during a warm subtropical climate. Alternation of lithologic units between carbonates and greenish mudrocks, and red mudstones and sandstones, suggests significant influence of climatic variations.

In the depocenter of the Potosí basin, the Upper Puca supersequence is underlain by the Miraflores Formation of Cenomanian–Turonian age. This unit consists of mostly marine limestones and subordinate marls, is less than 30 m thick, and was deposited during a tectonically quiescent period. The Miraflores transgression was the first to reach Bolivia since the Permian, and was related to the Cenomanian–Turonian global sea level high (Haq et al., 1987). The Miraflores–Upper Puca boundary is marked by the change from carbonates to pelitic mudrocks as predominant facies, accompanied by an abrupt increase of the sedimentation rate, and is estimated to be latest Turonian age (~89 Ma) (Jaillard and Sempere, 1991; Sempere, 1994).

Geographic distribution of the Upper Puca units indicates that, unlike the pre-Senonian deposits, sedimentation rapidly onlapped toward the external areas during this time interval. Depending on locality, the Upper Puca overlies Turonian, Cenomanian, or ?Albian strata (Jaillard and Sempere, 1991; Sempere, 1994); fluvio-eolian sandstones of Middle Triassic–Jurassic age (Ravelo, Yantata, or Beu formations) (Oller and Sempere, 1990; Sempere, 1995); locally deformed Paleozoic strata (mostly Ordovician and Silurian, and locally Devonian to Permian); or the Precambrian basement (in the northwest Altiplano). In the northwesternmost part of the Alto Beni Subandean belt and in the Santa Cruz area (Fig. 1), Cretaceous sedimentation began to onlap Jurassic deposits in late Campanian or Maastrichtian time.

During the Late Jurassic–early Oligocene interval, a large part of the wide Subandean-Llanura domain was covered by silcretes that developed upon the Jurassic Ichoa, Yantata, and Beu formations. These units were periodically gently uplifted and eroded when forebulges formed in response to shortening along the Pacific margin, and produced light-colored sands and clasts of silicified sandstone that were transported westward and northwestward into the basin. Such deposits are especially prevalent in early Maastrichtian and late Paleocene deposits (Sempere, 1994; and below).

The Upper Puca supersequence is normally overlain by the Cayara Formation, which is the lowermost unit of the Corocoro supersequence. This boundary is a significant unconformity, generally erosional and locally an-

gular (Marocco et al., 1987). Its age was known to be close to the Paleocene-Eocene boundary (Jaillard and Sempere, 1991) and thought to be possibly earliest Eocene (Marshall and Sempere, 1991); we demonstrate below that it is late Paleocene (58.2 Ma). This boundary marks the onset of Andean Bolivia functioning as a continental, external, "classic" foreland basin, probably resembling the present-day Chaco-Beni basin (Marshall and Sempere, 1991; Sempere et al., 1989). The overlying, partly equivalent Potoco and Camargo formations represent the corresponding late Paleocene–Oligocene basin fill and record the evolution of this foreland basin.

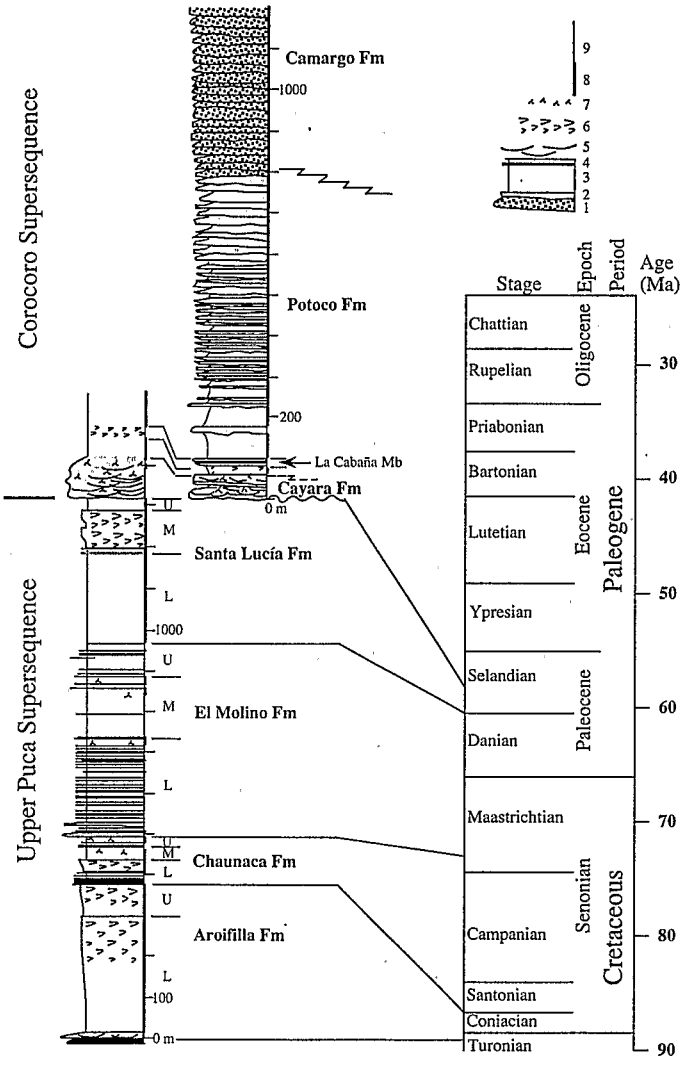

Figure 2. Stratigraphic columns illustrating rock types and thicknesses (same scale for both) of the Late Cretaceous to Eocene strata from parts of the Potosí basin. Data concerning the Aroifilla to Cayara formations are from the classic Miraflores syncline near Potosí. Because most of the Potoco-Camargo set is absent from the Miraflores syncline, data concerning these units are from the Camargo syncline (modified after Ponce de León, 1966). Abbreviations: Fm—formation, L—Lower, M—Middle, U—Upper. Lithologic symbols: 1—conglomerates and conglomeratic sandstones, 2—sandstones, 3—mudrocks, 4—carbonates, 5—channels, 6—evaporites, 7—rooting, 8—predominant brown-reddish color, 9—predominant greenish, grayish, or whitish, color. Time scale follows Cande and Kent (1992, 1995).

Upper Puca Stratigraphy (Latest Turonian–Early Selandian, ~89–58.2 Ma)

The Upper Puca supersequence is a 200–1200-m-thick sedimentary succession dominated by red mudstones, containing some conspicuous units consisting of green marls, fossiliferous limestones, and evaporitic bodies (Fig. 2). In the Potosí basin, the main Upper Puca units are the Aroifilla, Chaunaca, El Molino, and Santa Lucía formations (and their time equivalents). The fauna listed for this stratigraphic set includes continental and marine taxa (Gayet et al., 1991). On the basis of studies by Sempere et al. (1987, 1989), Jaillard and Sempere (1989), Jaillard et al. (1993), Sempere (1994), Gayet et al. (1993), and this paper, 11 sequences of regional stratigraphic value are currently recognized in the Upper Puca (Fig. 2).

Aroifilla Formation (Latest Turonian–Coniacian, ~89 to ~86 Ma). The Aroifilla Formation consists mainly of orange-red mudstones and subordinate evaporites and fine-grained red to green laminated sandstones, often with halite crystal casts. To the east, as at Maragua, thicker and more numerous red sandstone beds are intercalated in the Aroifilla mudstones, geographically forming a lateral transition with the Torotoro Formation, which crops out to the east. These facies are distributed in two sequences, namely the Lower Aroifilla (latest Turonian–early Coniacian) and the Upper Aroifilla (late Coniacian, and possibly earliest Santonian). The upper part of each sequence is significantly richer in evaporites and, in some specific areas, the upper Lower Aroifilla characteristically consists of a thick evaporitic body.

The evaporites in outcrops include gypsum beds, breccias, stratabound bodies, pink-brown gypsiferous mudstones, anhydrite nodules transformed to gypsum, and halite crystal casts and efflorescences. Gypsum facies indicate primary subaqueous precipitation as well as early diagenetic crystallization (Rouchy et al., 1993). Furthermore, an exploration well drilled a 2300-m-thick halite mass (very probably a diapir) south of Lake Poopó. Halite-bearing gypsum diapirs intruding Cenozoic strata are known in several areas of the Bolivian Altiplano, and might have remobilized evaporites from Aroifilla time-equivalent units.

Coarse sandstones or conglomerates (including mafic volcanic clasts) are locally present at the base of the Aroifilla and basaltic flows are interbedded in the Lower Aroifilla at several localities. Thin light green to white tuffaceous beds are known in several sections. The Aroifilla was deposited in a distal alluvial to salt-lacustrine (playa-lake) environment. Its thickness is highly variable, unlike the overlying Chaunaca Formation.

Chaunaca Formation (Santonian–Campanian, ~86 to ~73 Ma). Three sequences are recognized in the Chaunaca Formation: the Lower Chaunaca (Santonian), the Middle Chaunaca (early Campanian), and the Upper Chaunaca (middle and late Campanian, and possibly earliest Maastrichtian). Like the underlying Aroifilla, the Chaunaca was mainly deposited in distal alluvial to salt-lacustrine (playa-lake) environments but shows much less thickness variation than the Aroifilla.

The base of the Chaunaca Formation is conventionally the base of a 30-m-thick guide level, called the "basal limestone" of the Chaunaca, which consists of a fossiliferous intercalation of green marls, laminated gray limestones, and black shales (locally bearing galena or sphalerite crystals, and/or malachite or azurite stains), and yellow dolomites. Palynology indicates a Santonian to earliest Campanian age for this level (Pérez, 1987), in which the organic matter is of types II and III (Blanc-Valleron et al., 1994). Correlations with Peru suggest that it is early Santonian (Jaillard and Sempere, 1989). The upper part of the Lower Chaunaca consists of pink-brown gypsiferous mudstones (see Rouchy et al., 1993).

The Middle Chaunaca consists of red-brown mudstones that are bioturbated toward the top. The base of the Upper Chaunaca is a 15-m-thick level of green marls and thin limestones that resembles the basal limestone and is

called "upper green level." It correlates in Peru with a similar level of middle Campanian age. Because of its age, the upper green level is likely to be related to the middle Campanian global highstand (Haq et al., 1987). The upper part of the Upper Chaunaca consists of red-brown mudstones in which paleosols are increasingly frequent upward.

The two green levels, at the base of the Lower and Upper Chaunaca, are only present along the basin axis and thin out toward the west and east. Both mark transgressions of water bodies for which a restricted marine environment is favored. Both have similarities to the marine-influenced facies of the overlying El Molino Formation and correlate to similar marine guide levels in southern Peru, one of which yielded ammonites (Jaillard and Sempere, 1989; Sempere, 1994). The basal limestone has a marine bivalve and fish fauna (Gayet et al., 1993) and, in its lower portion, black shales, which are common at the base of marine transgressive deposits (Wignall, 1991). Because no particular sea-level high is known from the early Santonian, it is probable that deposition of the basal limestone was brought about by a sudden increase in tectonic subsidence (Sempere, 1994).

Facies in the five Aroifilla-Chaunaca sequences are arranged in the following order (type sequence): (0) sharp lithologic contact; (1) green marls, black shales and carbonates (more dolomitic toward the top); (2) brown-red mudstones with rare paleosols and/or evaporites; (3′) evaporite-bearing brown-red mudstones grading to evaporite beds, or (3″) brown-red mudstones with abundant rooted paleosols (occurrences of facies 3′ or 3″ depending on paleoclimate). This type sequence is interpreted as produced by (1) transgression of a restricted marine water body, and subsequent progressive regression, (2) establishment of very shallow lacustrine conditions evolving toward (3′) desiccation of concentrated brines and hypersaline waters under an arid climate, or (3″) immersion by progradation of distal alluvial facies with vegetation. Each of the five sequences is interpreted to have been deposited in all or some of these environments. The first three sequences end with the development of evaporites, whereas the last two end with the development of vegetated soils, suggesting change from a drier climate during Coniacian and Santonian time to a more humid climate in the Campanian. Superposition of the five Aroifilla-Chaunaca sequences is believed to have been controlled by variations in foreland subsidence, similar to that documented below for the Maastrichtian–Paleocene interval (Sempere, 1994).

Torotoro Formation (Coniacian–Campanian, ~87 to ~73 Ma). In the northeastern and southeastern parts of the Potosí basin, the Torotoro Formation is a sandy lateral equivalent of both the Aroifilla and Chaunaca formations deposited in fluvial and alluvial plain environments. It usually onlaps Paleozoic strata toward the northeast and southeast. The Torotoro locally includes conglomerates (with mafic volcanic clasts) in its basal portion and mostly consists of red-brown sandstones intercalated with subordinate red-brown siltstones and mudstones and frequent paleosols. Two levels of coalescent, rhizolith-rich paleosols established on brown-red argillaceous sandstones are conspicuous in the northeastern part of the basin. Because of their stratigraphic position and respective thicknesses, these two levels probably correlate with the two green levels of the Chaunaca Formation. Abundance of rooting at these two particular levels indicates biostasy in the continental

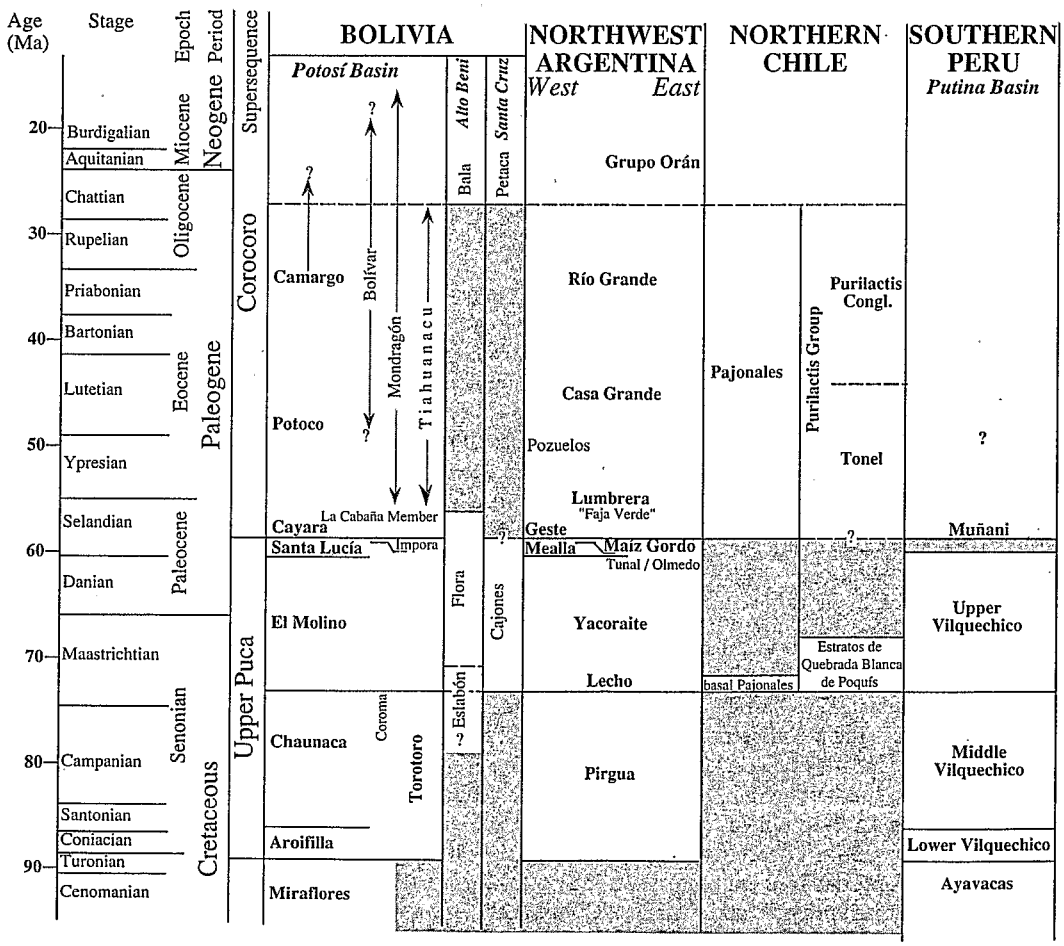

Figure 3. Regional correlation chart within the southern part of the Andean basin.

sedimentation area and appears to be related to the establishment of high-stand conditions in the basin axis, suggesting a correlation with the two transgressions recorded by the basal limestone and upper green level of the Chaunaca Formation (Sempere, 1994).

Coroma Formation (Campanian, ~78? To ~73 Ma). The Coroma Formation transitionally overlies the Chaunaca in the central Altiplano, west of the Senonian basin axis. Because it underlies the El Molino Formation, the Coroma is a lateral equivalent of the Upper Chaunaca Formation of the Potosí region. The Coroma consists of a thickening-upward intercalation of brownish and commonly rippled fine- to medium-grained sandstones and of red-brown mudstones identical to those of the underlying Chauna~It is coarser and thicker toward the west, and preliminary paleocurrent data suggest a western source for these sands. The Coroma Formation is interpreted to record progradation of fluvial sands from the west (Sempere, 1994).

El Molino Formation (Maastrichtian–Danian, ~73–60.0 Ma). The El Molino Formation and its equivalents have considerable extent in Bolivia and the central Andes (Fig. 4A). Its equivalents in Bolivia are, partly, the Eslabón and Flora formations of the Alto Beni Subandean belt, and the Cajones Formation of the Santa Cruz area (Fig. 3). Elsewhere its equivalents include the Upper Vilquechico Formation of southeast Peru (Jaillard et al.,

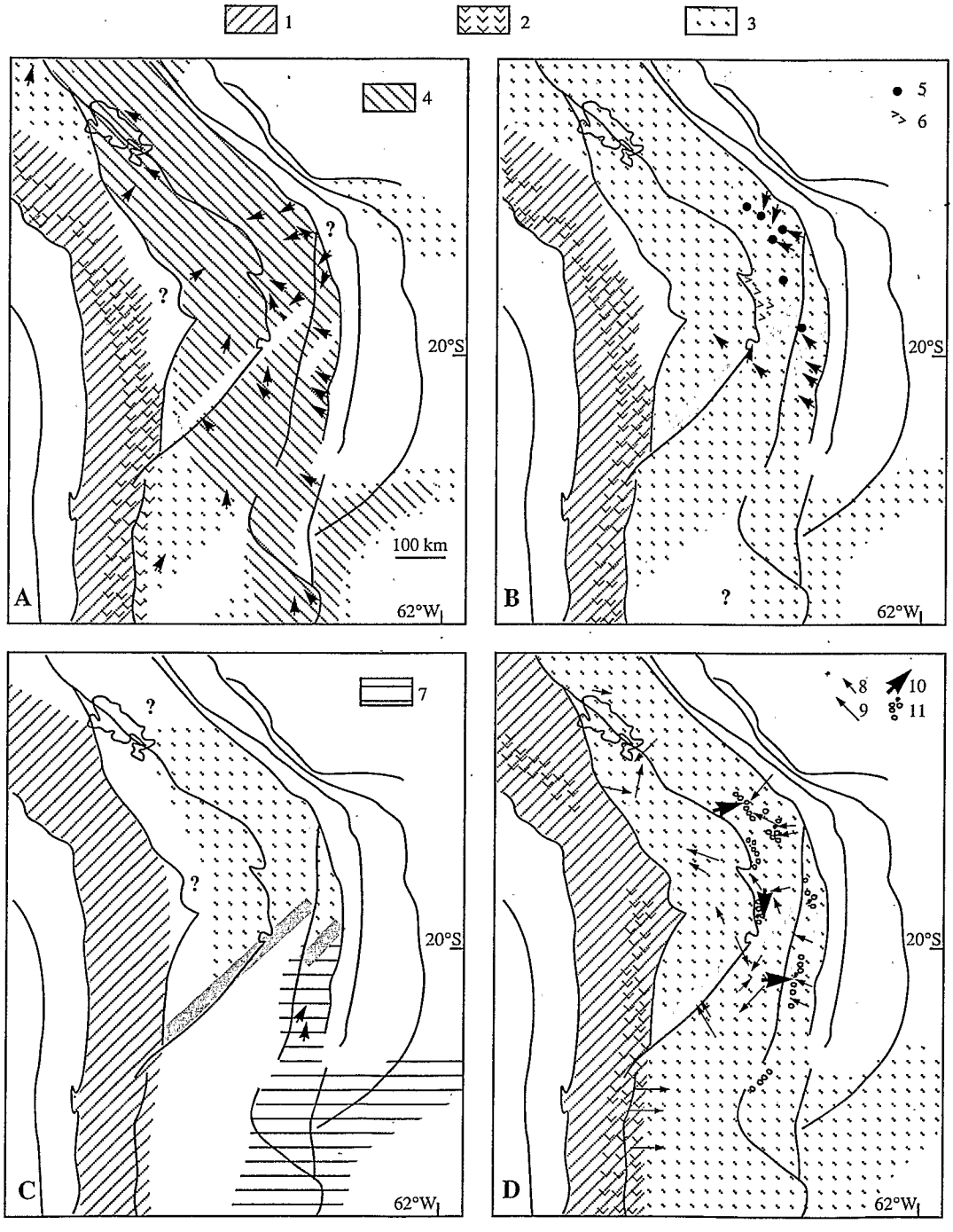

Figure 4. Maastrichtian to Eocene paleogeographies, on same structural background as in Figure 1. Shaded segments: Khenayani-Turuchipa paleostructural corridor. Arrows are mean paleocurrents; arrow tip is location of data. 1—Areas undergoing deformation, 2—magmatic arc, 3—extent of main basin. (A) Lower El Molino Formation (early and middle Maastrichtian), at approximate peak of marine influence (~71.5–70 Ma). 4—extent of marine influence. (B) Lower and Middle Santa Lucía Formation (60.0–58.5 Ma). 5—known occurrences of continental fossil vertebrates, 6—evaporites in Middle Santa Lucía. (C) Upper Santa Lucía and Impora formations (58.5–58.2 Ma). 3—Upper Santa Lucía subbasin, 7—Impora–Maíz Gordo subbasin. Darker patterns for the Khenayani-Turuchipa paleostructural corridor and western area undergoing deformation indicate higher tectonic activity. (D) Cayara, Potoco, and Camargo formations (late Paleocene to late Eocene or Oligocene). Paleocurrents: 8—Cayara, 9—Potoco and equivalents (apparent lack of a clear paleogeographic pattern is probably due to scarcity and strong diachroneity of data), 10—Camargo and Mondragón, 11—known outcrops of Camargo and Mondragón-Bolívar conglomerates.

1993), the Lecho, Yacoraite, Tunal, and Olmedo formations of northwest Argentina, and the Estratos de Quebrada Blanca de Poquís and the conglomeratic-sandy base of the Pajonales Formation of northern Chile (Fig. 3).

The El Molino Formation generally overlies the Chaunaca, Torotoro, or Coroma, which are partly equivalent formations (Sempere, 1994). The respective upper parts of these latter units are Campanian or earliest Maastrichtian and were deposited in a wide alluvial system where rooting was common. In contrast, the Lower El Molino facies were deposited in a subaqueous environment, which documents a significant transgression. The rich fauna and flora recorded for the El Molino Formation include continental and marine taxa (Gayet et al., 1991, 1993). Organic matter from the El Molino is of types II and III (Blanc-Valleron et al., 1994).

Abundant and sometimes varied marine fossils occur at numerous levels, indicating that the Maastrichtian–Danian central Andean foreland basin was periodically in connection with marine water. Marine fossils include dinoflagellates, calcispheres and nannoplanktonic microfossils, foraminifera, echinoids, serpulids, thick-shelled bivalves and gastropods, an operculum of ammonite (in southern Peru), flat-bodied selachians, and marine or estuarine actinopterygian fishes (Gayet et al., 1993; Sempere, 1994; Okamura and Mamani, 1994). Most of these marine fossil levels are located in the Lower El Molino. However, the depositional environment of the El Molino Formation was never openly marine, as indicated by the shallow and restricted marine facies and by the brackish to fresh-water fauna and flora that are also present, sometimes in abundance. Although strictly lacustrine environment was favored for the El Molino (e.g., Rouchy et al., 1993), it would be a surprising coincidence that a rapid lacustrine transgression, bearing a locally diversified marine fauna and flora, took place in Bolivia in the early Maastrichtian, at a time of global sea-level rise (Haq et al., 1987).

The Andean foreland basin was underfilled, flat and shallow, and the marine-influenced facies were deposited along its axis. Andean Bolivia and northwest Argentina (>500 000 km^2 if restored) were located in a "cul-de-sac" position at the extreme southern tip of the elongated Andean foreland basin, which probably connected with open marine waters only in present-day Venezuela, 3800 km to the north (Fig. 1). Major rivers were flowing into the basin from the east, south, and west, providing its flat and shallow southern part with fresh water and mud. The combination of these factors was responsible for the establishment of restricted-marine conditions (probably at least mesohaline) during portions of El Molino deposition and gave the environment some of its peculiar characteristics (Sempere, 1992, 1994; Gayet et al., 1993).

The El Molino Formation is usually 100–500-m-thick, and can locally reach 900 m. It consists of numerous facies that may have distinct stratigraphic distributions (Fig. 2). Green to gray and black, purplish, or brown-reddish mudstones or marls are the predominant facies in the basin, where they are intercalated with thin, fine- to coarse-grained limestone beds and very fine sandstones. White sandstones and oolite-bearing carbonates predominate, however, in the transgressive basal part of the formation.

Gray to light brown, micritic to bioclastic and/or oolitic limestones are present throughout the unit, although they are rare in the Middle El Molino. Thick and coarse oolitic bars are known in the Lower and Upper El Molino from along the basin margins in the Cochabamba and Camargo areas. Stromatolitic limestones (*Pucalithus* beds) are known from the marine-influenced portions of the Lower, basal Middle, and Upper El Molino (Fig. 5). Generally calcareous, clean and whitish, fine- to medium-grained sandstones are common in the lowermost part of the formation, where they sometimes form thick beds. Some sandstone beds are present in the upper Middle and middle Upper El Molino. Subemergent facies include some yellow dolostones or dolomitic fine-grained sandstones, which sometimes show cryptalgal laminations and mud cracks, and may be associated with dinosaur trackways. The abundance of sandstones and dolostones notably increases landward.

Paleosols are generally red-brown and many have root casts. Although some occur in the Lower and Upper El Molino, most are located in the Middle El Molino. Apart from recent gypsum produced by weathering of pyrite-rich rocks, the rare evaporite horizons consist of minor secondary gypsum, a few halite casts, and, in the uppermost El Molino, nodules or crystals replaced by calcite or silica (Rouchy et al., 1993). In the Camargo syncline, however, now-dissolved evaporites may have been present in the basal sandy portion of the El Molino and served as decollements for the widespread and spectacular east-verging tectonic duplexes in this region (see Kley, 1993); some gypsum crystal casts are present in these sandstones.

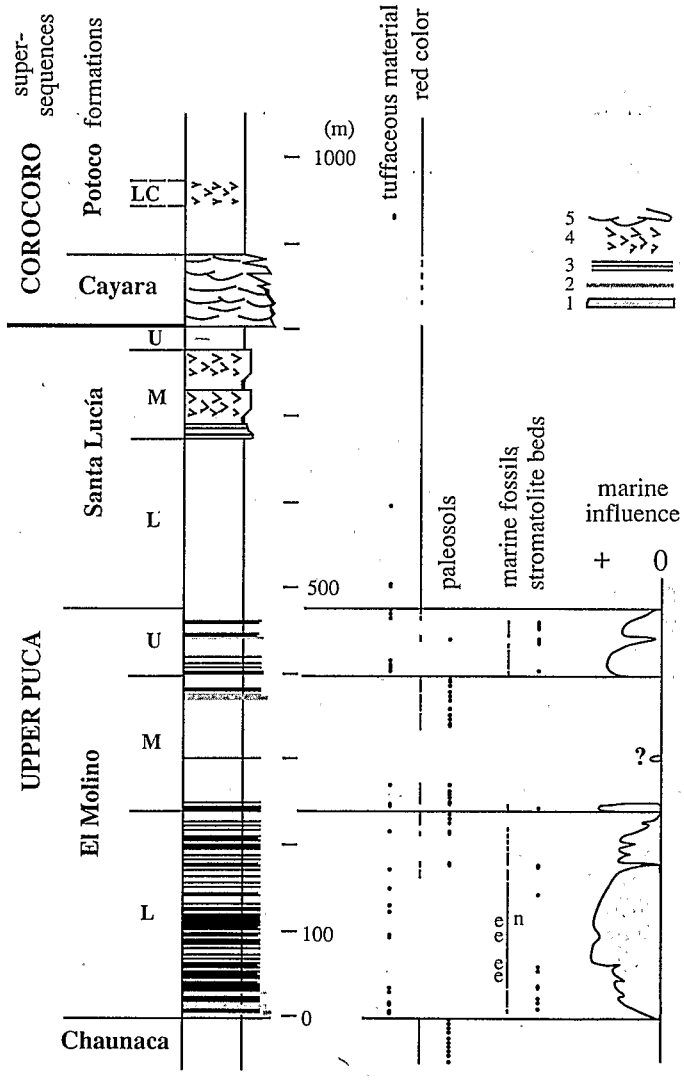

Figure 5. Summary of relevant stratigraphic data concerning the Upper Chaunaca through lower Potoco formations, based primarily on the La Palca stratotype in the Miraflores syncline near Potosí. Abbreviations: L—Lower, M—Middle, U—Upper; LC—La Cabaña member. Stratigraphic positions of known tuffaceous, marine fossil (e—echinoids, n—nannofossils), and stromatolite levels compiled from Bolivian parts of basin (modified after Gayet et al., 1993); distribution of red color and paleosols refers to La Palca section only. Marine influence curve deduced from facies and fossil data. Lithologic symbols: 1—sandstones, 2—mudrocks, 3—carbonates (mainly limestones), 4—evaporites (mainly gypsum), 5—channels.

Bright to light or dark green smectite-rich mudstones (Rouchy et al., 1993) are probably bentonites and some grade laterally into whitish to greenish altered tuffite beds where micas are visible. Well-crystallized smectite beds from the Lower El Molino (Rouchy et al., 1993) are reminiscent of subaqueous alteration of volcanic ash (Chamley, 1989). Analcime-rich beds in the uppermost El Molino (Rouchy et al., 1993) reflect alteration of volcanic products. Contribution of tuffaceous material to deposits of the El Molino Formation from the volcanic arc to the west was significant, especially in the Lower, lower Middle, and Upper El Molino, but is unknown in underlying Campanian strata (Fig. 5).

Along the basin axis, transgressive marine-influenced facies are present in the lower three-quarters of the Lower El Molino, at the base of the Middle El Molino, and in most of the Upper El Molino (Fig. 5). Marine carbonates and green to black mudstones generally yield some marine fauna or flora and indicate a shallow restricted-marine environment (Gayet et al., 1993). These facies are reminiscent of the basal limestone and upper green level of the Chaunaca Formation and of current models for transgressive facies (e.g., Wignall, 1991). Marine ingressions in this flat and shallow region of the Andean basin were controlled by the global eustatic level and a varying foreland subsidence rate, as documented below.

Marine-influenced fluctuations (Fig. 5) indicate that two principal transgressions of restricted-marine water bodies occurred during the El Molino depositional time: one is evident in the Lower plus basal Middle El Molino, and one is recorded by the Upper El Molino. These transgressions provide a correlation tool. Regressive fluctuations resulted in intercalations of shallower to terrestrial facies and paleosols, as in the uppermost part of the Lower El Molino. Terrestrial facies, mainly distal alluvial and lacustrine in origin and including numerous paleosols, accumulated during most of Middle El Molino time. The regression evidenced at the top of the Upper El Molino gave way to the development of a large lake system surrounded by a broad and flat alluvial landscape, in which the Lower member of the Santa Lucía Formation was deposited.

Santa Lucía Formation (60.0–58.2 Ma). The boundary between the El Molino and Santa Lucía formations is almost transitional. It can be traced throughout the basin and is expressed in northwest Argentina by the contact between the Yacoraite-Tunal-Olmedo beds and the Mealla Formation. The Santa Lucía and overlying units were deposited in alluvial to lacustrine environments. Distribution of the successive lakes remained controlled by the subsidence axis of the basin and by the Khenayani-Turuchipa paleostructural corridor (Figs. 1 and 4, B and C). The fauna and flora listed for the Santa Lucía Formation and overlying Lower Corocoro supersequence include only continental taxa (Gayet et al., 1991; Marshall and Sempere, 1991).

The Santa Lucía is divided into three stratigraphic sequences (Fig. 5). The Lower and Middle Santa Lucía form a coarsening and thickening-upward succession, which is the stratigraphic equivalent of the Mealla Formation in northwest Argentina (Fig. 3). The Lower Santa Lucía contains red-brown mudstones deposited in a lacustrine environment. Thin white to pink tuffaceous beds are present in this unit, especially in its basal portion, as in the Mealla Formation (Salfity and Marquillas, 1981). At Tiupampa on the basin margin, the Lower Santa Lucía consists of orange-brown bioturbated siltstones with common gastropod molds.

The Middle Santa Lucía begins with somewhat coarser facies. In the highly subsident Otavi area, lacustrine mudstones intercalate with slumped blocks and turbidites, which contain El Molino clasts as much as 1 cm in size. Along the basin margin, medium-grained to conglomeratic sandstones are intercalated with red-brown mudstones and paleosols and were deposited in meandering fluvial environments. These sandstones yield vertebrate remains at many localities, including Tiupampa (Figs. 1 and 4B). In the Camargo syncline, a thick paleosol occurs at the top of the Middle Santa Lucía sandstones, and a paleocurrent reversal perceptible in its northern segment indicates coeval reactivation of the nearby Khenayani-Turuchipa paleostructural corridor. The mud/sand ratio increases toward the interior of the basin. Near Potosí, the Middle Santa Lucía begins with sandy siltstones and mudstones and consists mainly of thickening-upward intercalations of gypsum beds. These evaporites have low $\delta^{34}S$ values suggesting some sulfur input of volcanic origin; they were deposited subaqueously in ephemeral or perennial brine ponds, and interstitially within their surrounding mud flats, through contraction of the lake system during a dry period (Rouchy et al., 1993). Evaporites were deposited in playa lakes scattered along the subsidence axis of the basin, as at Vilcapujio (Fig. 1).

The Upper Santa Lucía was also deposited in a lacustrine to alluvial environment (Fig. 4C). It consists of red-brown mudstones, which sometimes have thin green bands. The top of this unit is truncated by the erosional unconformity at the base of the Cayara Formation. The time equivalent of the Upper Santa Lucía southeast of the Khenayani-Turuchipa paleostructural corridor is the Impora Formation.

Impora Formation (58.5–58.2 Ma). The Impora Formation (Sempere et al., 1988) exists only southeast of the Khenayani-Turuchipa paleostructural corridor, in the Camargo syncline (Fig. 4C). It consists of purple to green lacustrine mudstones, marls and subordinate carbonates, and violet to white fluvial sandstones and conglomerates. Fossil vertebrates (fishes, turtles, crocodiles) are abundant (Gayet et al., 1991). Paleosols are common and most have horizons rich in calcareous nodules, which laterally grade into calcretes. Although it displays somewhat different facies, the Impora appears to be a time equivalent of the Upper Santa Lucía and seems to have been deposited in a distinct lacustrine basin separated from the Potosí region by contemporaneous reactivation of the Khenayani-Turuchipa paleostructural corridor (Sempere, 1994). However, carbonate-rich facies in the Upper Santa Lucía at Vilcapujio are reminiscent of the Impora Formation. Paleocurrents and clasts of the lower Impora conglomerates indicate that Mesozoic and Paleozoic rocks were eroding from an area southwest of the Camargo syncline (Marocco et al., 1987). The Maíz Gordo Formation of northwest Argentina contains greenish to purple, mudstone-dominated, vertebrate-rich (mostly turtles, crocodiles and fishes) facies and is similar to, and a distal equivalent of, the Impora Formation (Sempere, 1994) (Fig. 3). The Maíz Gordo is dated as late Paleocene on the basis of palynology (Volkheimer et al., 1984).

Lower Corocoro Stratigraphy (Late Selandian–Eocene, 58.2 to ? Ma)

The main units of the Lower Corocoro in the Potosí basin are the Cayara, Potoco, and Camargo formations (Fig. 2), which have local equivalents elsewhere in Bolivia and in adjacent areas. Because no detailed stratigraphy of these units has previously been published, we summarize here our present knowledge of these important formations. We also distinguish a new unit, the La Cabaña member, a light-colored intercalation in the lowermost part of the red Potoco Formation. Deposition of the Lower Corocoro succession occurred within a more proximal foreland setting than did sedimentation of the Upper Puca supersequence.

Cayara Formation (58.2 to ~57.8 Ma). The base of the Cayara Formation is an erosional unconformity in all Andean Bolivia (Sempere, 1994). This unconformity cuts through underlying units down to the Ordovician in the southwesternmost Cordillera Oriental and in a large area northwest of Potosí. The Cayara overlies the El Molino with marked angularity in one southeastern Altiplano locality (Marocco et al., 1987). The Cayara consists of whitish sandstones and minor mudstones and conglomerates which onlap from the west onto its basal erosional surface. The sandstones are fine to coarse grained and somewhat saccharoid, frequently finely bioturbated by roots, and distributed in channels that usually show trough cross-bedding. The thickness of the Cayara varies from a few meters to >150 m. The Cayara sandstones intercalate with subordinate red-brown mudstones,

forming a thinning and fining-upward succession that grades into the red-brown mudstones and siltstones of the lower Potoco Formation. The age of the Cayara-Potoco transition must therefore be diachronous.

The Cayara Formation was deposited in a wide fluviatile environment, >500 000 km^2 if restored. The fluvial network converged toward a basin axis which drained toward the north-northwest (Fig. 4D). Like the whitish sandstones present at the base of the El Molino Formation, the Cayara sands were probably eroded from Jurassic sandstones and overlying silcretes in the Subandean region, where a forebulge was uplifted in response to tectonic loading in the west. Evidence of extensive sediment transport and abundant vegetation, indicated by common rooting, suggests a warm and rainy climate.

Because the Cayara Formation overlies a conspicuous sequence boundary and displays characteristic whitish cross-bedded sandstone facies, it can be recognized throughout the central Andean basin. The Cayara is thus equivalent to at least the basal part of the Muñani Formation of southern Peru (Jaillard and Sempere, 1991), the light-colored cross-bedded sandstones generally occurring at the base of the Lumbrera Formation of northwest Argentina (Carbajal et al., 1977), the Geste Formation of the Argentine Puna (Jordan and Alonso, 1987), and the fluvial sandstones assigned to the Maíz Gordo Formation by Donato and Vergani (1988) in the Argentine Puna (Fig. 3). Some authors recognize a disconformity between the Lumbrera and the underlying Maíz Gordo formations (Gómez-Omil et al., 1989; Pascual et al., 1978), which supports the view that the Cayara and its equivalent strata were deposited irregularly on an erosional surface. However, apart from its basal sandstones, the Lumbrera Formation of northwest Argentina correlates with the lower part of the Potoco Formation of Bolivia. Mammal faunas of the Cayara and Lumbrera formations are summarized by Marshall et al. (1997).

Lower Potoco Formation and La Cabaña Member (~58.0 to ~55.5 Ma). The Potoco Formation transitionally overlies the Cayara Formation. Its lower part consists of thick red-brown mudstones deposited in a broad, flat, low-energy alluvial environment. The lower Potoco progressively grades into the middle Potoco, characterized by siltstone and sandstone intercalations that form a thickening- and coarsening-upward succession. The lower Potoco was long mistaken for the upper part of the Santa Lucía Formation in some areas of the Cordillera Oriental. Tuffaceous material in the lower Potoco is known only at Chita in a few thin beds.

The La Cabaña member is a light-colored intercalation commonly including evaporites that is present within the lowermost Potoco at most localities. This generally thin member is green, yellow-green, gray to violet, or whitish, and contrasts with the dominant red-brown of the lower Potoco mudstones. The La Cabaña member consists of green to purple marls or mudstones, gypsum nodules or beds, fine-grained carbonated sandstones (often bearing halite casts in the Altiplano), and rare medium- to coarse-grained channeled sandstones. Its thickness ranges from 0 or a few meters in southern Andean Bolivia to 60 m at La Cabaña (20 km east-southeast of Cochabamba) and more than 80 m in the Alto Beni Subandean belt, where it forms the upper part of the Flora Formation.

The northwest Argentine equivalent of the La Cabaña member is the Faja Verde ("green belt") present in the lower portion of the Lumbrera Formation (Salfity and Marquillas, 1981, 1994). The Faja Verde is generally as much as 25 m thick (Gómez-Omil et al., 1989), but may be twofold (Faja Verde Superior and Faja Verde Inferior) and collectively ~90 m thick in the local subsident part of the basin where palynology indicates a late Paleocene or early Eocene age (Carbajal et al., 1977; Quattrocchio, 1978b). The equivalent of the La Cabaña member in the Bolivian Altiplano is the Chuquichambi Formation, which consists mostly of evaporites that form diapirs and have operated as decollements of Neogene thrusts (e.g., west of Oruro). Deposition of the La Cabaña member occurred in a drier climate than that recorded by the typical red-brown rocks of the Potoco Formation. This explains the lack of fluvial drainage when compared with the abundance of channeling in the Cayara Formation. The La Cabaña evaporite levels formed in playa lakes scattered over the basin, while some major rivers (like that recorded at La Cabaña) continued to flow mainly toward the northwest or north-northwest. Thick lacustrine green marls and claystones are known in the upper Flora Formation in the Alto Beni Subandean belt. Lacustrine facies are also known from the Faja Verde in several localities of northwest Argentina. In the Otavi syncline, the La Cabaña member consists of thick lacustrine yellow and bluish marls and subordinate limestones. We believe deposition of the La Cabaña member and the Faja Verde occurred during a dry climatic period and that these units represent a synchronous sedimentary period and guide unit in the southern part of the Andean basin.

Potoco and Camargo Formations (~58.0 to ? Ma). The entire Potoco Formation consists of a thickening- and coarsening-upward succession of dominantly red-brown mudstones, siltstones, sandstones, and locally conglomeratic sandstones. These facies grade into the overlying Camargo Formation, which consists of thickening- and coarsening-upward sandstones, conglomeratic sandstones, and conglomerates intercalated with red-brown mudstones and siltstones (Fig. 2). The Potoco and Camargo are thus partly lateral equivalents and collectively form a 2000–5000-m-thick coarsening- and thickening-upward sequence interpreted to have been deposited as foreland basin fill (Marshall and Sempere, 1991; Sempere, 1990). Paleocurrent data suggest a drainage pattern during at least the early part of this depositional interval similar to that present during Cayara deposition (Fig. 4D).

In Bolivia, the Mondragón and Bolívar formations (see below), which crop out between Potosí and Cochabamba, are here recognized to be equivalents of the Potoco-Camargo. Another equivalent, in the northern Bolivian Altiplano, is the Tiahuanacu Formation, the top of which is dated as ~27 Ma (Sempere et al., 1990). Field observations allow correlation of the Potoco-Camargo set with equivalent strata in northern Chile and northwest Argentina (Fig. 3). The Potoco-Camargo sequence thickens toward the west in the western Bolivian Altiplano and in northern Chile, and thins toward the south in the Argentine Puna. Equivalent strata in northern Chile are most of the Purilactis Group (Salar de Atacama area), the Chojflias Formation (Poquís area), and almost the entire Pajonales Formation (excluding the dinosaur-bearing, basal conglomeratic sandstones) (Salinas et al., 1991). In northwest Argentina, its equivalents are the Lumbrera, Casa Grande, and Río Grande formations in the east (Pascual et al., 1978) and at least the lower part of the Pozuelos Formation in the west. The Potoco-Camargo strata correspond to red beds overlying the basal Muñani Formation and its Subandean equivalents in southern Peru.

The vertebrate paleontological data from northwest Argentine equivalents of the Potoco Formation were summarized by Pascual et al. (1981), Jordan and Alonso (1987), and Marshall et al. (1997) and suggest that the Potoco-Camargo was deposited during the late Paleocene–Eocene interval. Observation of some altered ignimbrite and andesite clasts in the upper Camargo suggests that the Camargo Formation probably ranges into the late Oligocene, because no such Cenozoic volcanic rocks are known in Bolivia before this time.

In the Camargo area, a northwest-derived conglomeratic bed as much as 1 m thick includes large El Molino clasts up to 10 cm and occurs just above the La Cabaña–lower Potoco lacustrine mudstones (i.e., at a low level in the Potoco section). This bed documents that the El Molino Formation was being eroded in a nearby tectonically uplifted source area as early as latest Paleocene or earliest Eocene time. No other conglomerates are known in the overlying 150 m of this section. The apparently west-derived Camargo conglomerates indicate a coeval uplift of Mesozoic and Paleozoic rocks west of their outcrop belt (Fig. 4D). The age of the Camargo conglomerates and of the responsible deformation, however, is poorly constrained.

Mondragón and Bolívar Formations (~58.0 to ? Ma). The Mondragón Formation consists of a thickening- and coarsening-upward succession dominated by reddish sandstones, conglomeratic sandstones, and minor conglomerates, with subordinate red-brown mudstone intercalations. It crops out mostly northwest of Potosí. Where the section is most complete, the Cayara Formation unconformably overlies the Lower El Molino or younger sequences; the Cayara Formation is conformably overlain by a 20-m-thick red mudstone unit similar to the lower Potoco, which in turn is conformably overlain by the 1000-m-thick Mondragón Formation. These relationships demonstrate that the Mondragón is a time equivalent of at least part of the Potoco-Camargo succession. In the same area, the Mondragón is gently folded into a broad syncline, which is unconformably overlain by distinctly folded ignimbrite flows of the early Miocene Agua Dulce Formation. Early Miocene ages are reported from volcanic tuffs intercalated in the easternmost outcrops of the Mondragón Formation (Evernden et al., 1977; Kennan et al., 1995); this eastern outcrop belt is believed to represent the eastward-onlapping, and thus the youngest, strata of the Mondragón-Bolívar basin. To the south (i.e., toward Potosí) the Mondragón Formation directly onlaps deformed Paleozoic and Cretaceous strata and is affected by a gentle deformation which mainly involves large-scale tilting.

The Bolívar Formation consists mainly of conglomeratic sandstones and conglomerates intercalated with red-brown mudstones and siltstones. It crops out in an area located north of the Mondragón depositional domain and unconformably overlies deformed Paleozoic and Mesozoic strata. The Mondragón and Bolívar formations are in adjacent areas and are believed to be partly lateral equivalents, and thus to be mainly of Eocene to early Miocene age. These units are interpreted to have been deposited as the infilling of the foreland basin of the Cabalgamiento Altiplánico Principal (Main Altiplanic thrust—CALP) thrust system (Fig. 1) (Sempere et al., 1991). Paleocurrent data suggest that this foreland basin was underfilled and axially drained to the south (Fig. 4D).

TABLE 1. $^{40}Ar/^{39}Ar$ LASER TOTAL FUSION ANALYSES OF SELECTED BIOTITE GRAINS FROM TUFFS OF THE LOWER MEMBER OF THE EL MOLINO FORMATION

L#	$^{37}Ar/^{39}Ar$	$^{36}Ar/^{39}Ar$	$^{40}Ar^*/^{39}Ar$	$^{40}Ar^*$	Age (Ma)	±1σ
M 21						
2913-04	0.01573	0.00426	1.9243	60.5	71.60	0.69
2913-05	0.00943	0.00481	1.9264	57.5	71.68	1.25
2913-06	0.02217	0.00670	1.9124	49.1	71.17	0.91
2913-07	0.03479	0.00494	1.9265	56.9	71.68	0.93
2913-08	0.03060	0.00390	1.9305	62.7	71.83	0.79
	Mean of five dates:				**71.59**	**0.25**
	Weighted mean (± std. error):				**71.60**	**0.22**
Contaminant grains?						
2913-03	0.0138	0.00465	1.9811	59.0	73.67	1.04
2913-10	0.0579	0.00388	1.9923	63.5	74.08	0.72
2913-02	0.0620	0.00235	2.2164	76.2	82.23	1.24
2913-09	0.0459	0.00145	10.7301	96.2	367.24	0.95
2913-01	0.0111	0.00042	15.1687	99.2	499.71	1.09
VCH-1						
7549-01	0.0185	0.00193	12.3219	95.6	72.77	0.22
7549-02	0.0054	0.00146	12.2828	96.6	72.55	0.19
7549-05	0.0057	0.00731	12.2568	85.0	72.40	0.27
7549-06	0.0058	0.00483	12.2071	89.5	72.11	0.22
	Mean of four dates:				**72.45**	**0.15**
	Weighted mean (± std. error):				**72.57**	**0.15**
Disturbed grains?						
7549-04	0.0716	0.01309	11.8477	75.4	70.03	0.26
7549-07	0.0070	0.02551	11.8505	61.1	70.04	0.49

Note: Irradiation monitor mineral: Fish Canyon Sanidine (27.84 Ma). $\lambda_e + \lambda_e' = 0.581 \times 10^{-10}\ yr^{-1}$; $\lambda_\beta = 4.962 \times 10^{-10}\ yr^{-1}$; $^{40}K/^{40}K_{total} = 1.167 \times 10^{-4}$ (from Dalrymple and Lanphere, 1971).
*Radiogenic.

ISOTOPIC DATING

Biotites from two tuffs in the Lower El Molino, exposed at a location (lat 20°05′S; long 66°54′W) about 5 km northeast of Chita on the road from Uyuni to Sevaruyo, were analyzed at the Berkeley Geochronologic Laboratories. The biotites and fluence monitors were irradiated in the Omega West research reactor at Los Alamos National Laboratory or the Triga reactor at the University of Oregon. Both irradiations were cadmium shielded. Following irradiation and bake-out, single mineral grains were fused with an Ar ion laser. The released gases were purified using SAES getters. Argon was analyzed with an online Mass Analyzer Product 215 noble-gas mass spectrometer. Sample fusion, gas purification, and mass spectrometry are fully automated. Procedural blanks were measured before beginning the analyses and after every third unknown, and they averaged less than 1.2×10^{-15} mol at m/e = 40.

Values for *J*, a parameter relating age to measured $^{40}Ar^*/^{39}Ar$ ratios as a function of the irradiation dose, were obtained from 6 to 10 replicate analyses of individual grains of coirradiated Fish Canyon Tuff sanidine. Ages were calculated using 27.84 Ma for the age of Fish Canyon Tuff sanidine (modified from Cebula et al., 1986). Corrections for interfering isotopes of Ar resulting from irradiation were determined for each reactor using calcium fluoride and a synthetic K-bearing glass; they are negligible for these samples. Mass discrimination was determined from analyses of air Ar using an online pipette.

Sample M21

Five total fusion analyses of single crystals of biotite from sample M21, located 19.8 m above the base of the El Molino at Chita, give a mean age of 71.59 ± 0.25 Ma (1σ). Five additional analyses of biotite from the same sample yielded ages that ranged from 74 to 500 Ma (Table 1). These older grains are interpreted to be nonjuvenile material, probably incorporated into the tuff during deposition and reworking.

Sample VCH-1

Four total fusion analyses of single crystals of biotite from sample VCH-1, located 3.8 m higher in the same section, give ages that are tightly clustered with a mean of 72.57 ± 0.15 Ma (1σ). The highly radiogenic Ar (radiogenic Ar = 85% to 95% of the total Ar) and tight reproducibility of these three analyses (Table 1) leads us to accept their mean as the best estimate of the age of this sample. Two additional crystals from this sample that have less radiogenic Ar yield ages of 70.03 and 70.04 Ma, distinct at the 1σ level from the four older crystals. We interpret these crystals to have undergone minor Ar loss or K gain during alteration.

Although the ages of the samples do not agree with their stratigraphic order, this difference is not considered significant. Applying the Critical-Value test of Dalrymple and Lanphere (1969), no difference in age between the two samples can be detected at the 95% level of confidence. Thus, the ages of the two samples are indistinguishable and their mean of 72.1 ± 0.5 Ma is the best estimate of the age of their stratigraphic level. On the basis of correlation of guide sequence boundaries and water-level fluctuations, these levels correlate to levels located ~29.0 m and ~34.2 m above the base of the El Molino in the La Palca section.

MAGNETOSTRATIGRAPHY

Details of the paleomagnetic collections, techniques, and data analysis are presented in the Appendix. In this section, we report magnetostratigraphic results.

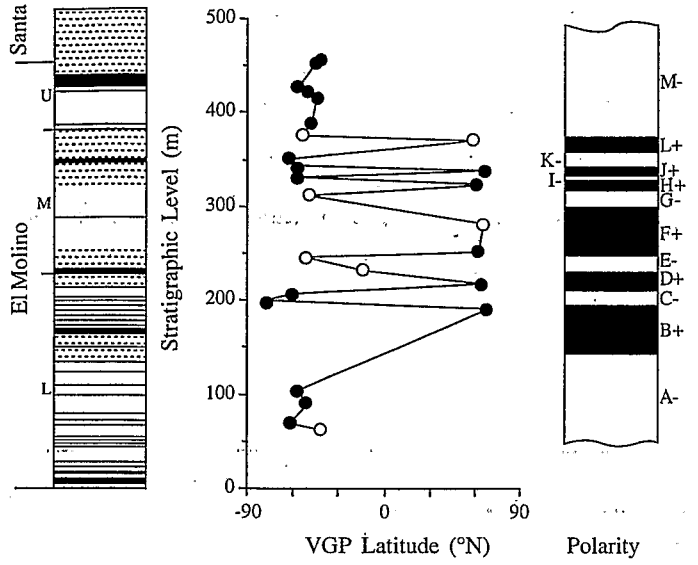

Figure 6. Polarity stratigraphy of La Palca section. Virtual geomagnetic pole (VGP) latitudes determined from site-mean characteristic components of natural remanent magnetization (NRM) directions listed in Table DR1 (see footnote 1 on p. 725) are plotted against stratigraphic level. Sites with at least three samples and clustering of sample characteristic components of NRM directions significant from random at the 5% significance level are shown by black circles; VGP latitudes for sites with only two samples yielding reliable characteristic components of NRM directions are shown by white circles. Interpreted magnetic polarity zonation and polarity zone designations are shown at the right. Black, normal polarity; white, reversed polarity. Symbols: black—limestones, dash—red mudstones dominant, dark stipple—coarse sandstones dominant, light stipple—fine sandstones dominant, white—green to gray or black mudstones dominant.

The magnetic polarity stratigraphy of the La Palca section is illustrated in Figure 6. Unfortunately, there are significant stratigraphic intervals from which no reliable paleomagnetic directions could be obtained and the magnetic polarity sequence lacks clear stratigraphic resolution of several polarity zone boundaries. In addition, several polarity zones are defined by a single paleomagnetic site and are not robust determinations. We do not regard the details of the sequence of polarity zones between the 150 and 375 m levels to be completely reliable. The conclusion, however, that this stratigraphic interval is dominated by normal polarity and records repeated geomagnetic polarity reversals is secure. There appears to be a reversed polarity zone of at least 50 m thickness at the base of the section and a reversed polarity zone of >100 m thickness at the top of the sampled section, proceeding into the base of the overlying Santa Lucía Formation at this locality. Correlation of the magnetic polarity sequence from the La Palca section with the geomagnetic polarity time scale is discussed below.

The magnetostratigraphic results from the Tiupampa and Sucusuma sections are illustrated in Figures 7 and 8, respectively. In both sections, all sites are of reversed polarity; correlations to the geomagnetic polarity time scale are discussed below. The magnetic polarity sequence from Pampa Grande in northwest Argentina is illustrated in Figure 9. Unfortunately, two polarity zones (B+ and C–) in this section are defined by results from single sites and must be considered provisional. Despite the generally low quality of the paleomagnetic data acquired and the minimal sampling density, the magnetic polarity sequence from Pampa Grande can be fit within a regional stratigraphy, when auxiliary information from lithostratigraphy, sequence stratigraphy, and biostratigraphy are considered.

MAASTRICHTIAN–PALEOCENE CHRONOSTRATIGRAPHY

Geochronology

All levels are located relative to the base of the El Molino Formation at La Pal~Correlation between the geomagnetic polarity time scale and the numerical time scale follows Cande and Kent (1992, 1995). The K-T and Campanian-Maastrichtian boundaries are thus respectively placed at 65 and 74.5 Ma (the latter may be as young as 72 Ma; Odin, 1994). A simple one-to-

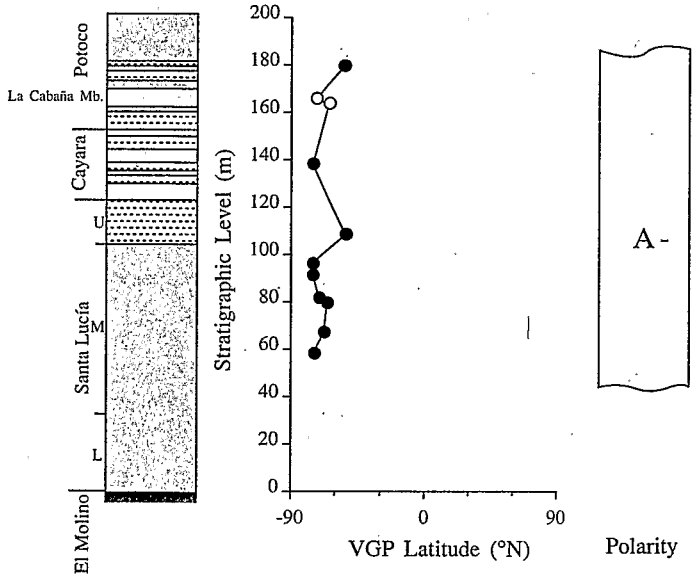

Figure 7. Polarity stratigraphy of Tiupampa section. Symbols as in Figure 6. Entire section is of reversed polarity.

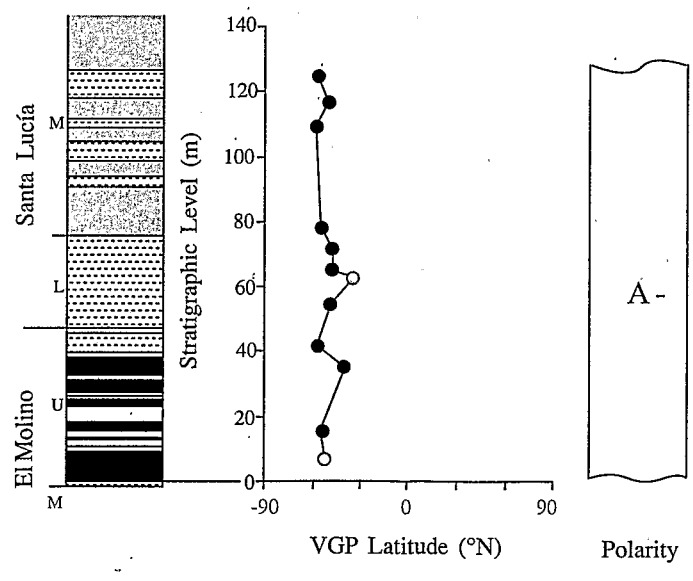

Figure 8. Polarity stratigraphy of Sucusuma section. Symbols as in Figure 6. Entire section is of reversed polarity.

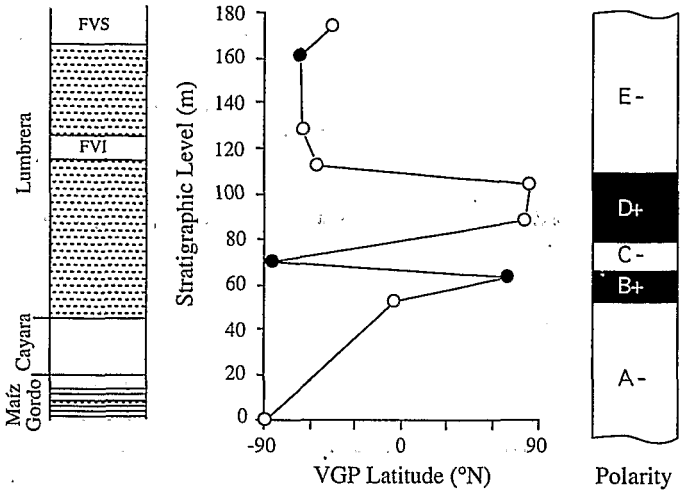

Figure 9. Polarity stratigraphy of Pampa Grande section, northwest Argentina. Symbols as in Figure 6. FVI—Faja Verde Inferior; FVS—Faja Verde Superior.

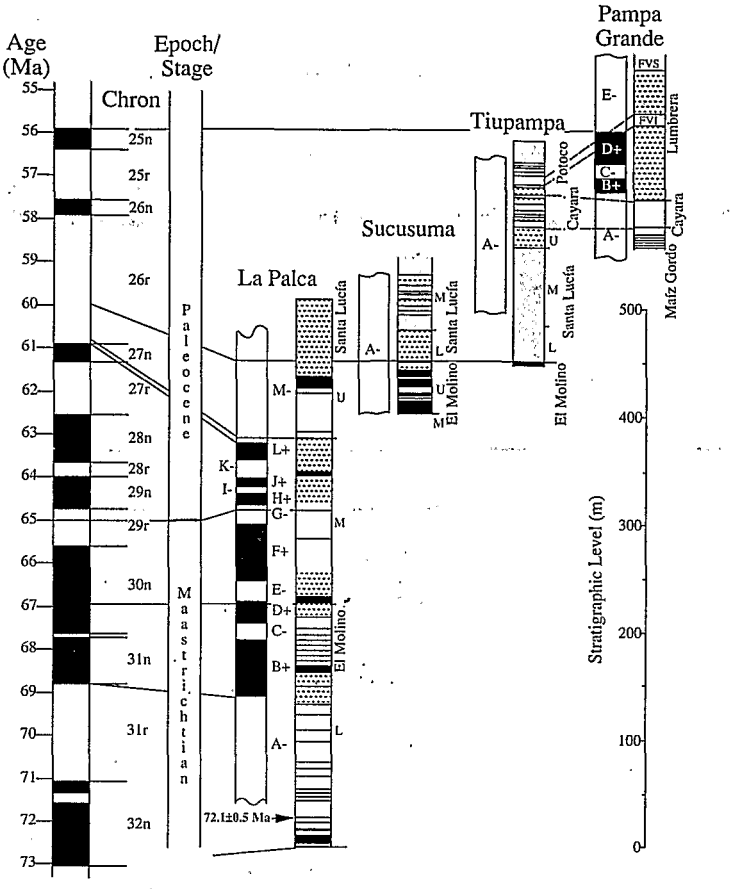

Figure 10. Correlation of magnetic polarity columns with geomagnetic polarity time scale. Isotopic date from within El Molino Formation is indicated in La Palca magnetic polarity column. Preferred correlations are indicated by dashed lines. Symbols as in Figure 6. FVI—Faja Verde Inferior; FVS—Faja Verde Superior.

one correlation of the La Palca polarity zonation to the geomagnetic polarity time scale is not evident (Fig. 10). The correlation shown in Figures 10 and 11 is our preferred interpretation because it is corroborated by the paleontologic data and agrees with a number of facts discussed below.

Correlations of magnetozone boundaries A–/B+ (~146.2 ± 42.7 m) and L+/M– (373.1 ± 2.6 m) at La Palca (Fig. 10) to the 31r/31n and 27n/26r chron boundaries of the geomagnetic polarity time scale, respectively, appear secure. This correlation implies ages of 68.7 Ma and 60.9 Ma for these two stratigraphic levels. The first site used in magnetostratigraphy (61.5 m) is in a reversed polarity zone correlated with chron 31r and thus younger than 71.1 Ma (base of chron 31r). This agrees with the isotopic date of 72.1 ± 0.5 Ma from the ~31.6 m stratigraphic level.

The Vivian Formation of Peru, which is partly equivalent to the basal sandstones of the El Molino Formation, yielded a Campanian palynologic assemblage (Jaillard and Sempere, 1989), suggesting that the base of the El Molino is close to the Campanian-Maastrichtian boundary. Emplacement of plutons in the Coastal batholith resumed at ~71 Ma at the latitudes of Bolivia (Soler et al., 1989), and reactivation of volcanism must have occurred earlier, as shown by our ~72.1 Ma tuffs. In several sections, tuffaceous material is present in the very base of the El Molino and is absent from the underlying Chaunaca, suggesting that the Chaunaca–El Molino contact records this reactivation of volcanism. On the basis of these data, we tentatively assign an ~73 Ma age to the Chaunaca–El Molino contact. This age might coincide with the Campanian-Maastrichtian boundary, which is between ~74.5 Ma (Cande and Kent, 1992, 1995) and 72 ± 0.5 Ma (Odin, 1994).

The Upper El Molino, the entire Santa Lucía, and apparently at least part of the Cayara formations were deposited during chron 26r, which spans the 60.9–57.9 Ma interval (Fig. 11). The regression marked by the El Molino–Santa Lucía contact is correlated with the Danian-Selandian boundary (60.0 Ma; Cande and Kent, 1992, 1995; Haq et al., 1987). This regression occurred at a time when no tectonic change is perceptible and was therefore apparently due to a eustatic effect.

The Lower Santa Lucía–Middle Santa Lucía contact is marked by an increase in grain size (Fig. 2). The age of this boundary is estimated to be ~59.5 Ma (Fig. 11). The contemporaneous increase in depositional rate suggests that tectonism and uplift were responsible for providing coarser material into the basin. This activity probably records the reactivation of the Khenayani-Turuchipa paleostructural corridor near the Middle Santa Lucía–Upper Santa Lucía boundary, which resulted in formation of the two lake systems represented respectively by the Upper Santa Lucía and Impora formations (Fig. 4C).

The erosional base of the Cayara Formation, near the end of chron 26r, is ~58.2 Ma and correlates with initiation of the first major sea-level lowstand in the Cenozoic (Haq et al., 1987). The position of the Cayara in the top of chron 26r is controlled by only one polarity site at Tiupampa (Fig. 7). At Pampa Grande (Figs. 9 and 10), the polarity data suggest that the Cayara occurs below the base of chron 26n, although the sampling is poor in this part of the section and the top of the Cayara may continue into chron 26n. Preliminary results from two Cayara sites near Camargo yield normal polarities at ~30 and ~45 m above the base of the Cayara. As noted above, the Cayara-Potoco transition is diachronous, so its age will predictably vary according to location in the basin. The two normal chrons from the lower part of the Lumbrera Formation are correlated with chrons 26n and 25n, and the Faja Verde Inferior occurs at the base of chron 24r (Figs. 9 and 10). The Faja Verde Superior is also in chron 24r and, assuming that deposition rates were constant for the lower Lumbrera, the top of the paleomagnetic section would be ~54.5 Ma (Fig. 10).

In summary, the ages of the sampled sequences would be as follows: Lower El Molino, ~73–66.9 Ma; Middle El Molino, 66.9–60.8 Ma; Upper

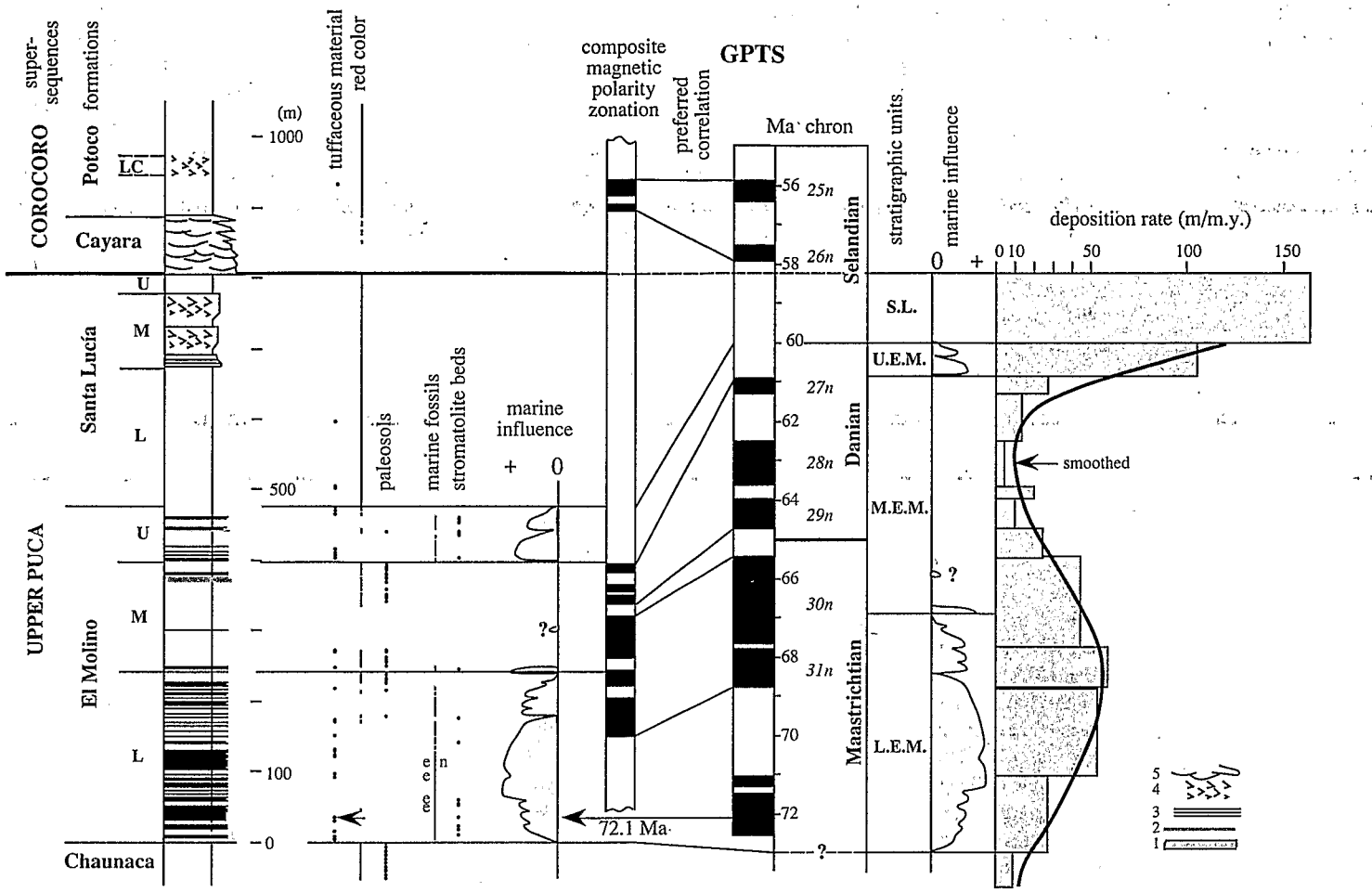

Figure 11. Summary of lithostratigraphic and chronostratigraphic data concerning the Upper Chaunaca through lower Potoco formations. Lithologic symbols and abbreviations as in Figure 5. Geomagnetic polarity time scale (GPTS) after Cande and Kent (1992, 1995). Deposition rates (undecompacted) for the El Molino–Santa Lucía interval at La Palca are believed to reflect subsidence rates because of homogeneity of facies and because burial depth exceeded 2500 m; deposition rates for younger units are not included because of scarcity of guide-levels and uncertainties in correlations. L.E.M.—Lower El Molino, M.E.M.—Middle El Molino, U.E.M.—Upper El Molino, S.L.—Santa Lucía.

El Molino, 60.8–60.0 Ma; Lower and Middle Santa Lucía (Mealla), 60.0–58.5 Ma; Upper Santa Lucía (Impora = Maíz Gordo), 58.5–58.2 Ma; Cayara (basal sandstones of Lumbrera), 58.2 to ~57.8 Ma; lowermost Potoco and La Cabaña member (lower Lumbrera and Faja Verde Inferior), ~58.0 to ~55.5 Ma (Fig. 11). These conclusions agree with the palynologic ages obtained in the Lower El Molino (Pérez, 1987), Tunal (Upper El Molino) (Quattrocchio et al., 1986), Maíz Gordo (Volkheimer et al., 1984), and Lumbrera formations (Quattrocchio, 1978a, 1978b).

Biostratigraphic Implications

The bed that yielded continental vertebrates at Pajcha Pata correlates to a level ~165 m above the base of the El Molino at La Palca and is thus ~68.4 Ma (Figs. 10 and 11). This bed is the lowest level in the El Molino Formation, which has a diverse continental fauna, including coelurosaur, snake, various amphibian, lungfish, numerous fish, and unpublished mammal remains (Marshall, 1989; Rage et al., 1993). Correlation of paleontologic data to the reference section at La Palca indicates that dinosaur trackways are unknown above the upper Lower El Molino (~202 m) and that Cretaceous fishes are unknown above the basal Middle El Molino (~236 m) (Gayet et al., 1991). According to our preferred correlation to the geomagnetic polarity time scale, these levels would be ~67.5 and ~66.7 Ma, respectively. Our correlation constrains the location of the K-T boundary to within ~43 m of section at La Palca, between levels ~281 m and ~324 m. This interval is in the middle part of the Middle El Molino and at La Palca shows lacustrine facies.

The Tiupampa mammals were collected in the middle part of the Middle Santa Lucía (Marshall and Muizon, 1988; Gayet et al., 1991; Muizon, 1991; Marshall et al., 1997) and are thus ~59.0 Ma. Revision of the mammal faunas from Argentina and Bolivia provides a consistent view of the Paleocene mammal biostratigraphy and evolution in the Andean basin (Marshall et al., 1997).

Minimum ranges of some ostracod species collected in the Chaunaca and/or El Molino formations (Camoin et al., 1991; Gayet et al., 1993) are as follows: *Candona huaitracoensis*, Santonian–early Maastrichtian; *Ilyocypris* aff. *triebeli*, early Maastrichtian; *I.* aff. *wichmanni*, early Maastrichtian–latest Danian. Nannofossils assigned to *Calculites ovalis* and *C. obscurus* were recovered from 120 m above the base of the El Molino Formation at La Palca (Okamura and Mamani, 1994) and are early Maastrichtian (~70 Ma). Dinocysts assigned to *Apectodinium homomorphum* and *A. quinquelatum* were

recovered from the Upper El Molino at La Palca (Blanc-Valleron et al., 1994); although the latter species indicates a late Selandian–Ypresian age in the North Atlantic and northwest Europe, the Bolivian dinocysts are latest Danian according to our chronostratigraphy.

Numerous charophytes, identified as *Feistiella gildemeisteri* by J. Dejax, M. Feist and N. Grambast-Fessard, were recovered from the basal Upper Santa Lucía at Tiupampa, which dates them as ~58.5 Ma. The charophytes are not reworked because they occur throughout a 1-m-thick level that is laterally continuous over several hundreds of meters. This species is also common in reportedly Maastrichtian units in southern Peru (Jaillard et al., 1993). Charophytes (*"Tectochara" ucayaliensis oblonga*) reputedly indicating a middle or late Eocene age (Branisa et al., 1969) or a Paleocene–Eocene age (Mourier et al., 1988) were collected (L. Branisa, 1985, personal commun.) from above the La Cabaña member in the lower part of the Potoco Formation, which was long mistaken for a part of the Santa Lucía Formation in the Camargo area. These fossils are thus of latest Paleocene or earliest Eocene age. Fossil leaves collected from the La Cabaña member at La Cabaña, and currently being studied by J. Dejax (Muséum National d'Histoire Naturelle, Paris) are latest Paleocene in age.

Eustasy and Subsidence

Bolivia and northwest Argentina were located in the southern intracontinental "cul-de-sac" part of the underfilled Andean foreland basin, where ingressions of marine water were possible at times of sea-level highs and sufficient subsidence. Because global sea level was high during most of Senonian to Danian time (Haq et al., 1987), tectonic effects are required to explain why only a part of the succession shows a marine influence. For example, the Campanian is represented in Bolivia by mostly continental deposits and paleosols, whereas it is a time of high eustatic level. The Maastrichtian–Danian is a period of high eustatic level, yet only the early Maastrichtian and latest Danian of Bolivia record a marine influence. Most of the late Maastrichtian–Danian is of continental origin and commonly shows paleosols. Thus, marine-influenced facies in the El Molino Formation indicate that tectonic subsidence was high enough to permit marine ingression whereas continental facies and paleosols suggest that subsidence was low (however, paleosols are also to be expected in a high-subsidence context at times of major sea-level lows). A correlation of marine-influenced portions of the section with high subsidence and deposition rate, and paleosol-rich continental portions with low subsidence and deposition rate, is expected. Our preferred correlation shows this relationship in a general sense and in some detail (Fig. 11).

The boundary between the Lower and Middle El Molino is identified by the base of a thin marine-influenced level within a dominantly continental portion where well-developed paleosols are abundant. According to our preferred correlation, the age of this boundary is ~66.9 Ma and the paleosol zones are ~67.2–66.9 Ma and ~66.7–66.4 Ma, which is in some agreement with the sharp and short sea-level lowstand recognized by Haq et al. (1987) at ~68 Ma, especially if the boundaries of the Maastrichtian are 1–2 m.y. younger than assumed by these authors (Odin, 1994). Maximum inundation was achieved in the central Andean area at ~71.5–70 Ma (Fig. 11), which may represent the maximum flooding surface recognized by Haq et al. (1987) as ~73.5 Ma.

TECTONIC IMPLICATIONS AND SUMMARY

Volcanic Activity

Tuffaceous material is abundant in the Lower, lower Middle, and Upper El Molino, and Lower Santa Lucía (Fig. 11), suggesting that volcanic activity in the coastal arc was important during the intervals from ~73 to ~66 Ma and from 60.8 to 59.5 Ma. The apparent absence of volcanic-derived sediments from the units underlying the El Molino indicates that volcanic activity was low between ~86 to ~73 Ma. The Chaunaca–El Molino and Middle El Molino–Upper El Molino boundaries (~73 and 60.8 Ma, respectively) were thus accompanied by a significant increase in volcanic activity, which seems to have been reduced between ~66 and 60.8 Ma and after 59.5 Ma. These data agree with the evolution of the coastal magmatic arc: At the latitudes of Andean Bolivia, pluton emplacement apparently stopped at ~84 Ma, resumed at ~71–70 Ma, and significantly decreased at ~59 Ma (Soler et al., 1989). In central Peru, plutonism apparently stopped at ~78 Ma, resumed at ~75 Ma, and stopped again at ~59 Ma (Soler and Bonhomme, 1990).

Tectonic History

Central Andean tectonic evolution (Fig. 12) is usually considered to have begun with a Late Jurassic–Early Cretaceous extensional to transtensional episode associated with the initiation of rifting between South America and Afri~Prior to Turonian time, tectonic conditions were dominated by extensional to transtensional conditions, interrupted along the Pacific coast by occasional compressional to transpressional events. The tectonic regime was controlled by large-scale wrench faulting that affected the western margin and built some proto-Andean reliefs (Jaillard, 1994). No true foreland basins, however, are known in the central Andes before the Turonian.

Latest Turonian–Early Coniacian Rifting. After a tectonically quiescent interval in the Cenomanian and Turonian, widespread extensional conditions were abruptly established at ~89 Ma in the Potosí basin and adjacent northwest Argentina. Rifting during latest Turonian–early Coniacian time is evidenced by the erosional unconformity at the base of the Aroifilla (Jaillard and Sempere, 1991), abundant basic magmatic conglomerate clasts and occasional volcanic flows in the Lower Aroifilla, narrow troughs in which the basalts are located and elongated playa lakes established in these downwarped areas, and the major thickness variations of the Lower Aroifilla (Sempere, 1994). Subsequent evolution of the basin as a distal part of the Andean foreland suggests that this latest Turonian–early Coniacian extensional episode represents a regional destabilization produced by the onset of shortening along the Pacific margin at ~89 Ma.

Coniacian–Campanian. The Upper Aroifilla and subsequent sequences point to a different tectonic setting. There is a marked contrast between the thickness irregularity of the Lower Aroifilla and the more consistent thickness of the Upper Aroifilla to Upper Chaunaca succession. These sequences onlap upon the external areas; each follows a regressive pattern and shows an overall decrease in subsidence rate, which is accompanied by progradation of clastic material from the west (Coroma Formation). The conjunction of these phenomena is reminiscent of aspects of evolutionary models of foreland basins (Flemings and Jordan, 1989, 1990). These observations suggest that the Potosí basin was functioning as the distal part of the Andean foreland basin during the Coniacian–Campanian interval and that compressional tectonism, involving shortening and loading of the South American lithosphere, had started on the Pacific margin (Sempere, 1994). Thus, infilling of latest Turonian–early Coniacian tensional structures was accompanied or followed by onlap of distal foreland sedimentation toward areas that had remained devoid of Cretaceous deposits.

Maastrichtian. After relative quiescence in the Campanian, tectonic activity along the margin was reactivated at ~73 Ma. Documentation of a significant tectonic episode initiated in early Maastrichtian time is provided by an abrupt increase in sedimentation rate at the Chaunaca–El Molino boundary, a rapid shift of the basin axis toward the west, and deposition of the lowermost El Molino sands derived from the east and southeast. This episode

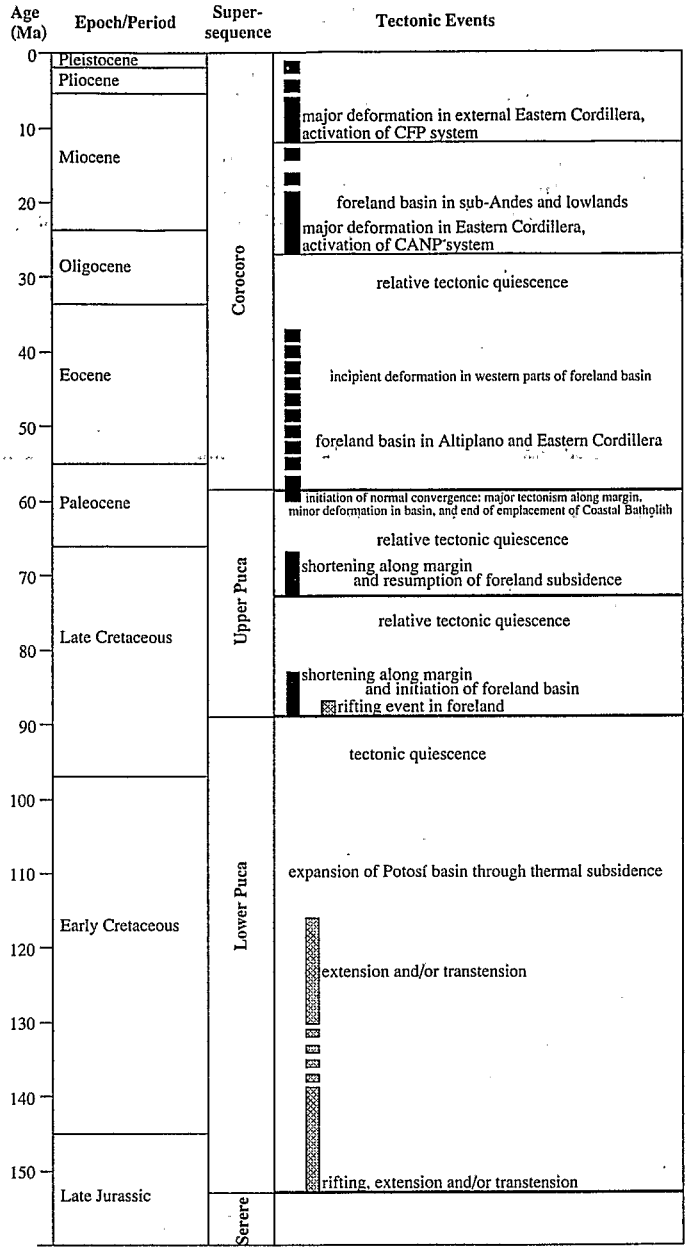

Figure 12. Summary chart showing tectonic events in the Potosí basin.

produced a sharp increase in the rate of deformation and tectonic loading along the coastal areas, which resulted in high tectonic subsidence in the foreland. Subsidence in this underfilled basin was maximum between ~71 and ~66 Ma (Fig. 11), which enhanced the effects of the early Maastrichtian global marine transgression. Although longitudinal subsidence was controlled at a large scale by tectonic loading in the west, local subsidence occurred along the northwestern edge of the Khenayani-Turuchipa paleostructural corridor.

Paleogene. Subsidence decreased during the late Maastrichtian, was low during the Danian, but increased again in the latest Danian, and peaked in the early Selandian (Fig. 11). This increase in foreland subsidence again reflects reactivation of major shortening and tectonic loading along the margin. This tectonic event developed mostly between 59.5 and 58.2 Ma and correlates with the end of emplacement of the Coastal batholith in Peru (Fig. 12). It produced folding in southwestern Bolivia (Marocco et al., 1987), gentle deformation southeast of Vilcapujio, reactivation of the Khenayani-Turuchipa paleostructural corridor, synsedimentary deepening of the Otavi lake, and widespread deposition of coarser sediments, including conglomerates and lacustrine turbidites containing El Molino clasts. These phenomena are postdated by the widespread erosional unconformity at the base of the Cayara Formation. This 58.2 Ma unconformity records in Bolivia a substantial modification of the tectonic setting, including forebulge uplift (generating the Cayara sands) and westward migration of the subsidence axis (Fig. 4, C and D). This event marks the onset of a continental foreland basin in Andean Bolivia that was infilled during the latest Paleocene–Oligocene by the thick Potoco and Camargo formations. As early as Eocene time, however, this basin underwent internal deformation in the southern Altiplano and west of the Camargo Formation outcrop belt (Fig. 4D), as well as northwest of Potosí, as documented by the Mondragón Formation.

Eocene Deformation. The Mondragón and Bolívar formations represent the infilling of the foreland basin of the CALP thrust system (Fig. 1). Because these units were previously interpreted as late Oligocene–early Miocene, major activity of the CALP–Khenayani fault thrust system, including the Ticatica duplexes and Calazaya nappe, was believed to be of this age (Baby et al., 1992; Sempere et al., 1991). However, because of the chronologic evidence presented above, this age interpretation is no longer tenable. Although chronologic data for the upper Potoco and Camargo formations still lack precision, it is evident that the CALP–Khenayani fault system was active mainly in the Eocene. In turn, activation of the San Vicente fault and subsequent tectonic development in the southern Altiplano, also interpreted previously as late Oligocene–early Miocene (Baby et al., 1990), must be mainly of Eocene age.

Although only a few paleocurrent determinations are available, namely from the Morochata (Kennan, 1993) and Camargo synclines, the Camargo conglomerates are apparently derived mainly from the west, which indicates a coeval uplift of Mesozoic and Paleozoic rocks west of its outcrop belt. For example, late Oligocene–early Miocene rocks directly overlie the Ordovician in the Tupiza area (Hérail et al., 1992), although the Late Cretaceous–Paleocene rocks are known to have been deposited there, and it is likely that this erosion started in the Eocene.

Along both flanks of the Camargo syncline, east-verging duplexes involve shallow decollements in the basal Lower El Molino. These duplexes predate the formation of the syncline, which was produced by thrust deformation involving deep decollements located in strata older than Middle Ordovician. Because this younger deformation is believed to represent the major Andean tectonism initiated in the late Oligocene (Sempere et al., 1990), it is possible that the shallow-level duplexes formed in Eocene and/or Oligocene time. The structural style they imply and the relative shallowness of their decollement suggest that the Camargo area resembled the present-day Subandean belt during the Eocene–Oligocene. As suggested by our preliminary paleocurrent data from the Camargo area, the Camargo conglomerates might have been deposited in longitudinal valleys between ridges formed by stacked anticlines.

Regional Tectonic Correlations

The Late Cretaceous–Tertiary tectonic history of the central Andes, although distinctive in certain aspects, has many parallels with the tectonic history of other parts of the Andes. At most latitudes along the Andean margin, extension and subsidence prevailed during the Late Jurassic–Early Cretaceous. A transition to a compressive continental margin, where foreland basins developed inboard, began with the opening of the South Atlantic. In southernmost South America, the large extensional back-arc basins (Magallanes and Neuquén) changed to foreland basins beginning in the mid-

Cretaceous (Wilson, 1991; Winslow, 1982, Vergani et al., 1995), earlier than this same transition in the central Andes. In central and northern Peru, the subsiding continental margin converted to a western-sourced foreland basin at ~89 Ma (Jaillard, 1994), corresponding to the tectonic transition in the central Andes.

Reconstructions of the Pacific basin suggest that a triple junction, at the end of a spreading ridge between the Phoenix and Farallon plates, moved southward along the Andean margin from the Central American region to Antarctica from about 100–110 Ma to 80–75 Ma (Cole, 1990). After this ridge passed southward, the Farallon (later Nazca) plate subducted under the western margin of the South American plate. Initiation of the foreland basins in the central Andes apparently occurred after the South American and Farallon plates were in contact across this subduction zone. After ~80–75 Ma, most of the western margins of both North and South America were in contact with the Farallon plate (or later pieces of it) and, in addition, both the North American and South American plates were moving generally westward at about the same rate due to spreading at the Mid-Atlantic ridge. Because of these similarities, the two plates underwent analogous relative plate motions and changes in motions along their western margins that likely account for the correspondence between tectonic events of these margins (see below) during the Late Cretaceous and early Tertiary.

The relative motion between the Nazca and South American plates is known directly from ~70 Ma (anomaly 31) (Pardo-Casas and Molnar, 1987; Pilger, 1984), and variations in relative motion can account for aspects of tectonic episodes in the central Andes, as well as along the Andean margin in general. The relative motion was obliquely convergent during deposition of the El Molino and Santa Lucía formations, the distal foreland basin strata in the central Andes. The sequence of continental and marine strata seen during this interval in the central Andes is closely matched in coeval foreland basin sequences in the Subandean regions of northern Peru, Ecuador, and into Colombia, thus suggesting a similar and nearly synchronous tectonic transition. For example, in the Oriente of Ecuador, the Maastrichtian–Paleocene Tena Formation contains early Maastrichtian marine levels mixed with continental and brackish-water strata, and it unconformably overlies the mid- to Upper Cretaceous sequence (Dashwood and Abbotts, 1990; Kennerley, 1980).

At about 56–57 Ma (anomaly 25), the convergence rate between the Nazca and South America plates increased substantially, and the ensuing interval of fast and nearly perpendicular convergence continued into the early Oligocene (~35 Ma) (Pardo-Casas and Molnar, 1987; Pilger, 1984). The Cayara-Potoco-Camargo (and Mondragón-Bolívar) sequence and the 58.2 Ma unconformity record this episode of fast convergence in the central Andes. Along the entire Andean margin, many rock units and unconformities also indicate a substantial change in depositional patterns, arc magmatism, and deformation, which correlate with this increased rate of convergence. Coarser and typically continental foreland basin Paleocene–Eocene or Eocene sequences unconformably to paraconformably overlie the Maastrichtian–Paleocene sequences in Andean and Subandean regions of Peru, Ecuador, and Colombia (Jaillard, 1994; Dashwood and Abbotts, 1990; Schamel, 1991), and magmatic complexes of this age range are extensive in the coastal regions in the northern, central and southern Andes (Mégard, 1989; Ramos, 1988; Richards, 1995). Although the details of the ages of the units and unconformities vary, this episode of fast convergence correlates to major tectonism throughout the Andes.

CONCLUSIONS

The latest Cretaceous–early Paleogene units of Bolivia appear to be reliably dated. The El Molino and Santa Lucía formations respectively span the ~73–60.0 Ma and 60.0–58.2 Ma intervals. The base of the Cayara Formation is 58.2 Ma.

The early Andean evolution of Bolivia comprises three main tectonic periods: latest Turonian–Campanian (~16 m.y. long), Maastrichtian–early Selandian (~15 m.y. long), and middle Selandian–early Oligocene (~31 m.y. long) intervals. These three periods began with a tectonic event produced by (re)activation of tectonic loading along the margin, represented by the respective bases of the Aroifilla (~89 Ma), El Molino (~73 Ma), and Cayara (58.2 Ma) formations.

The ~89 Ma tectonic event marked a turning point in Andean evolution at these latitudes. Compressional building of the central Andes was initiated at that time (Sempere, 1994) and since then, foreland conditions have prevailed in the eastern Andean domain.

The ~59.5–58.2 Ma tectonic event documented above shortly predates a significant increase in convergence rate and achievement of nearly perpendicular convergence of the Nazca and South American plates at about anomaly 25 (Pilger, 1984; Pardo-Casas and Molnar, 1987), i.e., ~55.9–57.6 Ma (Cande and Kent, 1995). It marks the initiation of "classic" continental foreland sedimentation in Andean Bolivia. The thick late Paleocene–Oligocene Andean foreland fill records significant internal deformation of this foreland basin during its evolution, as conjectured by Kennan et al. (1995). The Cayara-Potoco-Camargo succession is lithologically reminiscent of the Chaco succession of the Subandean-Llanura domain, which represents the late Oligocene–Holocene fill of the current Andean foreland basin (Sempere, 1990, 1991; Sempere et al., 1990).

Stratigraphic evidence for late Paleocene–Oligocene deformation in Andean Bolivia permits a better understanding for the Paleogene rotations documented by Butler et al. (1995). These rotations were almost certainly the result of rotations between crustal domains separated by thrust and strike-slip faults. They are likely to reflect an early stage of development of the Bolivian orocline.

Comparisons with North America

The Phanerozoic geologic evolution of the central Andes and of North America, especially the western United States, share an increasing number of similarities (Sempere, 1995). Among them is the major activation of thrusting in the Sevier thrust belt at ~89 Ma (DeCelles, 1994), which matches the coeval initiation of compressional building of the central Andes. The Senonian–early Paleocene underfilled foreland basin of the Andes is reminiscent of the Western Interior Seaway, reflecting similarities in early Cordilleran-type geotectonic evolutions. The tight synchroneity, at ~58.5–58.2 Ma, of the Upper Puca–Corocoro and Zuñi-Tejas sequence boundaries (see Leighton and Kolata, 1991) is a major, and unexpected, result of our study. The tectonism dated as early late Paleocene in the central Andes is thus apparently roughly synchronous with the Laramide orogeny. The Corocoro supersequence of Bolivia equates with the Tejas sequence of North America, and both are divided into two subunits with a boundary at ~27 Ma (Haq et al., 1987; and this study). These chronological coincidences suggest that the Late Cretaceous–Holocene histories of the Pacific margins of both continents were controlled by related causes.

ACKNOWLEDGMENTS

Acknowledgment is made to the donors of the Petroleum Research Fund, administered by the American Chemical Society, for partial support of this research. Aspects of this study were supported by UR 1H of Orstom (Institut Français de Recherche Scientifique pour le Développement en Coopération); the National Geographic Society (grants 2467-82, 2908-84, 3381-86, and 4810-92); Gordon Barbour Fund; Department of Geological and Geophysical Sciences, Princeton University; National Science Foundation (grants EAR-88-04423, EAR-90-17382, and EAR-9316414); Ministère de

la Recherche, France (1994); and an Action Spécifique (1983–1989) from the Muséum National d'Histoire Naturelle, Paris; a grant from the University of Arizona International Program Development Fund; and Yacimientos Petrolíferos Fiscales Bolivianos (YPFB). We thank J. Dejax, T. Fiorillo, P.-Y. Gagnier, M. Gayet, E. Jaillard, A. Lavenu, C. de Muizon, J. Oller, B. Sigé, M. Suárez-Riglos, R. Suárez-Soruco, and C. Winker. We also thank Bryan Backes, David Lindsay, Thurston Strom, and Rob Feyerharm for assistance with paleomagnetic laboratory analyses. We acknowledge the helpful reviews provided by James Reynolds and Keri Kodama.

APPENDIX

Paleomagnetic Collections, Methods, and Analysis

At least three paleomagnetic samples were collected from each of 150 sedimentary horizons (paleomagnetic sites) distributed among four stratigraphic sections (three in Bolivia, one in northwest Argentina) of the El Molino Formation and/or overlying continental deposits. Samples were either cored in situ with standard paleomagnetic core drilling equipment or were collected as oriented hand samples, which were later trimmed into paleomagnetic specimens for measurement. Paleomagnetic samples were collected from the finer grained layers and are dominantly reddish claystones and siltstones. Following sample preparation, all paleomagnetic specimens were stored, measured, and demagnetized in a magnetically shielded room with average field intensity less than 200 nT (nannotesla). All measurements of natural remanent magnetization (NRM) were done using a two-axis cryogenic magnetometer (ScT C-102). A few samples were subjected to alternating-field (AF) demagnetization, but this treatment generally was ineffective in separating components of NRM. Following initial NRM measurements, pilot specimens from all sites were subjected to progressive thermal demagnetization to determine the unblocking temperature spectra for the NRM. Progressive thermal demagnetization employed from 8 to >16 temperature steps up to 680 °C. The magnetic field inside the thermal demagnetization furnace was less than 10 nT.

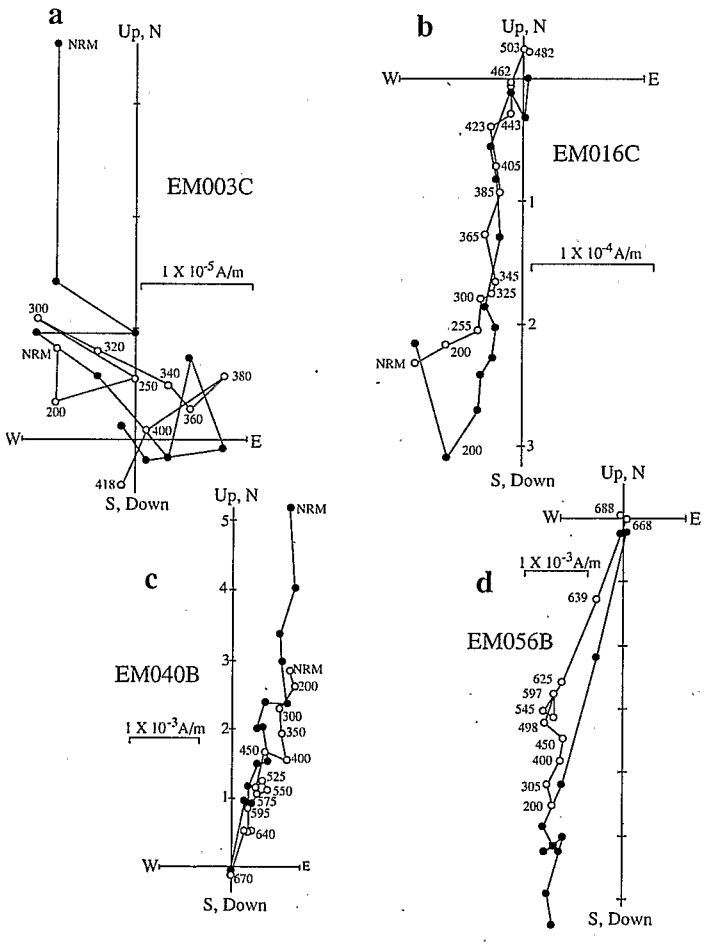

Figure A1. Vector end-point diagrams showing representative thermal demagnetization behavior of samples from the La Palca section. Black circles are projections onto the horizontal plane. White circles are projections onto the vertical plane. Numbers adjacent to data points indicate temperature (°C) of thermal demagnetization. Directions are shown in geographic (in situ) coordinates.

Results of thermal demagnetization were analyzed by plotting vector end-point diagrams in order to identify linear segments of demagnetization trends. The corresponding components of NRM were determined using principal component analysis (Kirschvink, 1980) to fit line segments to linear trends of vector end points. For characteristic components of natural remanent magnetization (ChRM), the origin of the vector component diagram was used as an additional independent datum in the principal component analyses. Results are discussed in detail below, but the general data selection criteria are outlined here. Only characteristic components of natural remanent magnetization determined by results of at least four successive thermal demagnetization steps and for which principal component analysis yields a maximum angular deviation (MAD) ≤15° are considered reliable. As discussed below, many samples do not satisfy these criteria. Applying these stringent selection criteria, however, allows attention to focus on the best determined characteristic components of NRM. For the majority of samples meeting these criteria, results from ≥6 thermal demagnetization temperatures usually yield line fits with maximum angular deviation ≤10° and often yield maximum angular deviation ≤5°. Relaxing the selection criteria does not significantly affect the results and only introduces undesirable noise into further levels of analysis.

Other selection criteria involve within-site comparison of characteristic components of NRM directions using standard Fisher (1953) statistics. For sites with three samples (N = 3) which yield acceptable characteristic components of NRM, only those sites with clustering of characteristic components of NRM directions significant from random at the 5% significance level are accepted for further analysis (Watson, 1956). For N = 3, this criterion requires a vector resultant, R, ≥ 2.62. For sites with N = 2 ChRM directions, site-mean characteristic components of NRM directions with R ≥ 1.8 are considered acceptable. All site-mean characteristic components of NRM directions meeting these criteria are used for analysis of magnetic polarity zonation. For tectonic analysis of paleomagnetic directions, a more stringent selection criterion is applied. Only site-mean directions with 95% confidence limit, α_{95}, ≥ 20° are admitted for tectonic analysis. This criterion requires that the within-site concentration parameter (Fisher et al., 1987), k, is greater than 35 for N = 3 directions. This is a stringent criterion, but application of more permissive criteria does not significantly affect the results and only introduces larger confidence limits in the results.

La Palca. The stratigraphic section at La Palca (lat 19.53°S, long 294.17°E; Fig. 1) is the type section of the El Molino, Santa Lucía, and Cayara formations (Lohmann and Branisa, 1962). The sampled section has a total thickness of 480 m, within which 62 paleomagnetic sites were collected. Samples from this section provided the poorest quality paleomagnetic results, because the basal portion of the section is dominated by restricted-marine limestones and brackish-water deposits. NRM of samples from these rocks was almost invariably of low intensity (NRM < 10^{-4} A/m), and often responded to thermal demagnetization in an erratic fashion. Figure A1A illustrates this erratic behavior from which no characteristic components of NRM can be identified. Sites failing to yield characteristic components of NRM directions were concentrated in the lower half of the La Palca section. Fewer than half of the sites collected in this section provided characteristic components of NRM directions that pass the selection criteria for magnetic polarity determination.

Figure A1B illustrates thermal demagnetization behavior of a sample from one of the few sites in the Lower El Molino Formation that yields a reliable site-mean direction. Unblocking temperatures (T_{UB}) are dominantly between 200 and 500 °C suggesting that magnetite is the dominant carrier of natural remanent magnetization. Although the NRM direction is somewhat erratic at the higher temperature steps, the characteristic components of NRM direction are reasonably well defined. Demagnetization behavior of a red-brown paleosol sample from the Middle El Molino is shown in Figure A1C. The illustrated behavior with a small, yet significant, fraction of characteristic components of natural remanent magnetization apparently carried by hematite with unblocking temperatures approaching 680 °C is typical of well-behaved samples from the upper half of the El Molino Formation. Demagnetization of NRM for a red-brown mudstone sample from the Upper El Molino is shown in Figure A1D. The line segment used to determine the characteristic components of NRM direction for this sample is defined by the progression of vector end points resulting from thermal demagnetization at ≥625 °C; this component is entirely carried by hematite.

Site-mean directions that pass the above outlined selection criteria for magnetic polarity determinations are listed in Table DR1[1], both in geographic (in situ) and stratigraphic (corrected for bedding tilt) coordinates. The La Palca section is a homoclinally tilted succession in the southeast edge of the Miraflores syncline. The small variations in bedding attitudes do not allow application of the fold test for paleomagnetic stability, although a reversals test (discussed below) is positive. Characteristic components of NRM directions (of either normal or reversed polarity) are apparently carried at some sites by magnetite and at other sites by hematite. We interpret characteristic components of NRM directions carried by magnetite as depositional remanent magnetizations (DRM), and characteristic components of NRM directions carried by hematite as chemical remanent magnetizations (CRM). Sites with characteristic components of NRM carried by magnetite occur stratigraphically adjacent to sites with characteristic components of NRM carried by hematite and within the same polarity zone. These observations suggest that CRM components carried by hematite were formed soon after deposition, although the possible time interval between deposition and acquisition of CRM is not actually known. Possible time lags between deposition and acquisition of CRM could account for the lack of simple one-to-one correlation between magnetic polarity zones in the La Palca section and the geomagnetic polarity time scale.

Tiupampa and Sucusuma. At Tiupampa (lat 18.0°S, long 294.5°E; Fig. 1), a stratigraphic succession of ~200 m thickness was measured from the base of Santa Lucía Formation through the Cayara Formation and into the base of the overlying Potoco Formation. C. Winker collected 17 paleomagnetic sites in 1985 from the middle ~120-m-thick portion of this section. Typical thermal demagnetization behavior of samples from the Santa Lucía portion of the section is illustrated in Figure A2A. The characteristic component of NRM has unblocking temperatures distributed from ~400 to >650 °C, indicating that a significant portion of the characteristic magnetization is carried by hematite. Figure A2B illustrates more erratic, but still acceptable for magnetic polarity determination, behavior for a sample from the Cayara Formation.

The sampled section at Sucusuma is about 6 km north of Torotoro (18.08°S; 294.25°E; Fig. 1). The section has a thickness of ~130 m, from which 28 paleomagnetic sites were collected in a stratigraphic sequence through the Upper El Molino into the overlying Santa Lucía. The success rate in retrieving reliable characteristic components of NRM directions was much better for samples from the Santa Lucía Formation, which is dominated by fine-grained red sediments than for samples from the predominantly restricted-marine El Molino deposits. Figure A2, C and D, illustrates thermal demagnetization behavior of two Santa Lucía samples from this locality. The unblocking temperatures of the characteristic components of NRM in most cases extend to >580 °C, indicating a significant contribution from hematite. Nevertheless, a colinear component of NRM with unblocking temperatures below 580 °C suggests that magnetite is also a carrier of NRM. This latter component is most likely of depositional origin. The fundamental agreement in direction of the components of NRM carried by hematite and by magnetite suggests that the CRM carried by the hematite in the strata of the Sucusuma section was acquired soon after deposition. Site-mean parameters of characteristic components of NRM for the stratigraphic sections at Tiupampa and Sucusuma are listed in Tables DR2 and DR3, respectively (see footnote 1).

Pampa Grande. We collected 12 paleomagnetic sites from what was mapped by Carbajal et al. (1977) as the lower half of the Lumbrera Formation in a stratigraphic succession of ~180 m thickness at Pampa Grande in northwest Argentina (lat 25.8°S, long 294.6°E; Fig. 1). These collections and paleomagnetic analyses were done in 1977, when laboratory techniques were less rigorous than those applied to the collections described above from Bolivia. Although the results are less reliable than those reported above, we include the results from Pampa Grande because of their importance to the regional stratigraphic synthesis discussed above.

All samples collected from the Lumbrera Formation were oriented hand samples. Lithologies collected were either green or red claystones and siltstones which were often fissile, difficult to collect, and sometimes disintegrated during handling in the laboratory. Red samples were unaffected by AF demagnetization and were subsequently demagnetized using thermal demagnetization at several temperatures up to 600 °C. The NRM component remaining after thermal demagnetization is interpreted as a CRM, most likely acquired near the time of deposition. Green rocks responded to AF demagnetization, and that technique was used to remove low-coercivity components of NRM in an attempt to isolate the characteristic components of NRM of presumed depositional origin. Demagnetization to 20 or 30 mT effectively removed low-coercivity NRM components that were generally aligned with the present geomagnetic field at the sampling locality.

[1]GSA Data Repository item 9719, Tables DR1–DR4, is available on request from Documents Secretary, GSA, P.O. Box 9140, Boulder, CO 80301. E-mail: editing@geosociety.org.

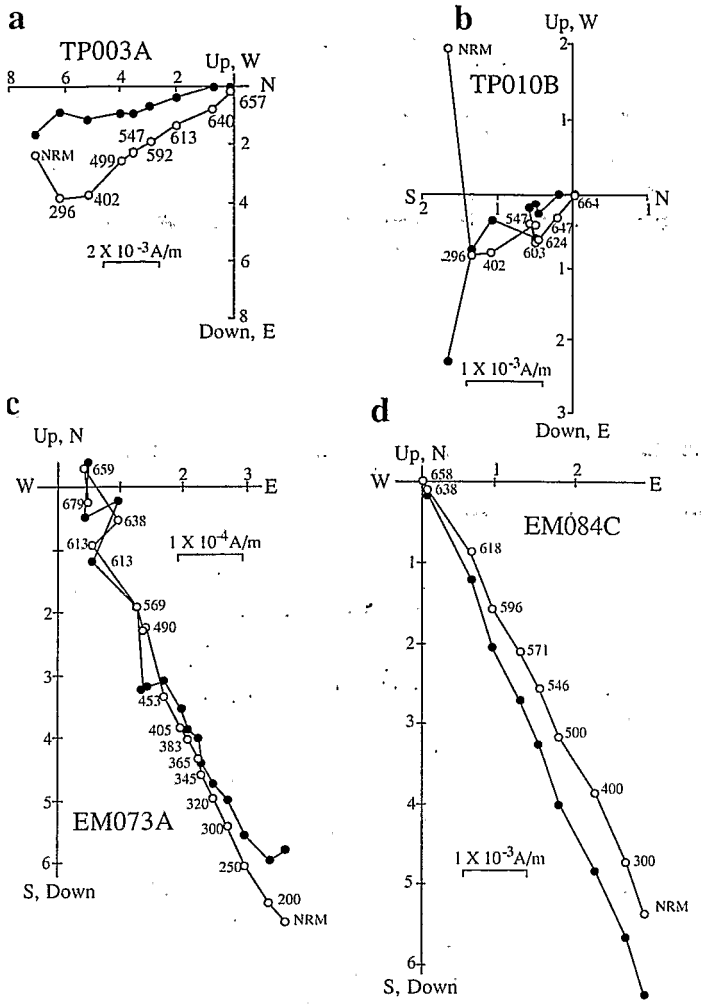

Figure A2. Vector end-point diagrams showing representative thermal demagnetization behavior of samples from Tiupampa section (A, B) and Sucusuma section (C, D). Symbols as in Figure A1.

Demagnetizations were not done at a sufficient number of steps to allow meaningful principal component analysis. Accordingly, site-mean directions listed in Table DR4 (see footnote 1) are the result of "blanket" AF or thermal demagnetizations. Samples from two sites had NRM intensities too low ($<10^{-5}$ A/m) for confident identification of characteristic components of NRM. For several sites, only two specimens survived the demagnetization process; for one site, only a single specimen yielded a characteristic component of NRM of sufficient intensity to confidently determine the direction.

REFERENCES CITED

Baby, P., Sempere, T., Oller, J., Barrios, L., Hérail, G., and Marocco, R., 1990, Un bassin en compression d'âge oligo-miocène dans le sud de l'Altiplano bolivien: Paris, Comptes Rendus de l'Académie des Sciences, sér. II, v. 311, p. 341–347.

Baby, P., Sempere, T., Oller, J., and Hérail, G., 1992, Evidence for major shortening on the eastern edge of the Bolivian Altiplano: The Calazaya nappe: Tectonophysics, v. 205, p. 155–169.

Blanc-Valleron, M.-M., Schuler, M., Rauscher, R., Camoin, G., and Rouchy, J.-M., 1994, La matière organique des séries d'âge Crétacé supérieur–Tertiaire inférieur du bassin de Potosí (Cordillère orientale, Bolivie): Apports stratigraphiques et paléogéographiques: Paris, Comptes Rendus de l'Académie des Sciences, sér. II, v. 319, p. 1359–1366.

Branisa, L., Grambast, L., and Hoffstetter, R., 1969, Quelques précisions nouvelles, d'après les charophytes, sur l'âge du Groupe Puca (Crétacé–Paléocène, Bolivie): Compte Rendu Sommaires des Séances de la Société Géologique de France, v. 8, p. 321–322.

Butler, R F., Richards, D. R., Sempere, T., and Marshall, L. G., 1995, Paleomagnetic determinations of vertical-axis tectonic rotations from Late Cretaceous and Paleocene strata of Bolivia: Geology, v. 23, p. 799–802.

Camoin, G., Rouchy, J.-M., Babinot, J.-F., Deconinck, J.-F., and Tronchetti, G., 1991, Dynamique sédimentaire et évolution paléogéographique d'un bassin continental en position d'arrière-arc: Le Maastrichtien de la Cordillère Orientale (Bolivie): Paris, Comptes Rendus de l'Académie des Sciences, sér. II, v. 315, p. 891–896.

Cande, S. C., and Kent, D. V., 1992, A new geomagnetic polarity time scale for the Late Cretaceous and Cenozoic: Journal of Geophysical Research, v. 97, p. 13917–13951.

Cande, S. C., and Kent, D. V., 1995, Revised calibration of the geomagnetic polarity timescale for the Late Cretaceous and Cenozoic: Journal of Geophysical Research, v. 100, p. 6093–6095.

Carbajal, E., Pascual, R., Pinedo, R., Salfity, J. A., and Vucetich, M. G., 1977, Un nuevo mamífero de la Formación Lumbrera (Grupo Salta) de la comarca de Carahuasi (Salta, Argentina): Edad y correlaciones: Publicaciones del Museo Municipal de Ciencias Naturales "Lorenzo Scaglia," Mar del Plata, v. 2, p. 148–163.

Cebula, G. T., Kunk, M., Mehnert, H. H., Naeser, C. W., Obradovich, J. D., and Sutter, J. H., 1986, The Fish Canyon Tuff, a potential standard for the $^{40}Ar/^{39}Ar$ and fission-track methods: Terra Cognita, v. 6, p. 139–140.

Chamley, H., 1989, Clay sedimentology: Berlin, Springer, 623 p.

Cole, G. L., 1990, Models of plate kinematics along the western margin of the Americas: Cretaceous to present [Ph.D. dissert.]: Tucson, University of Arizona, 461 p.

Dalrymple, G. B., and Lanphere, M. A., 1969, Potassium-argon dating: San Francisco, California, W. H. Freeman, 258 p.

Dashwood, M. F., and Abbotts, I. L., 1990, Aspects of the petroleum geology of the Oriente Basin, Ecuador, *in* Brooks, J., ed., Classic petroleum provinces: London, Geological Society, p. 89–117.

DeCelles, P. G., 1994, Late Cretaceous–Paleocene synorogenic sedimentation and kinematic history of the Sevier thrust belt, northeast Utah and southwest Wyoming: Geological Society of America Bulletin, v. 106, p. 32–56.

Donato, E., and Vergani, G., 1988, Geología del área de San Antonio de los Cobres: Boletín de Informaciones Petroleras, v. 15, p. 83–101.

Evernden, J. F., Kriz, S. J., and Cherroni, C., 1977, Potassium-argon ages of some Bolivian rocks: Economic Geology, v. 72, p. 1042–1061.

Fisher, N. I., Lewis, T., and Embleton, B. J. J., 1987, Statistical analysis of spherical data: Cambridge, United Kingdom, Cambridge University Press, 329 p.

Fisher, R. A., 1953, Dispersion on a sphere: Proceedings of the Royal Society of London, ser. A, v. 217, p. 295–305.

Flemings, P. B., and Jordan, T. E., 1989, A synthetic stratigraphic model of foreland basin development: Journal of Geophysical Research, v. 94, p. 3851–3866.

Flemings, P. B., and Jordan, T. E., 1990, Stratigraphic modeling of foreland basins: Interpreting thrust deformation and lithosphere rheology: Geology, v. 18, p. 430–434.

Gayet, M., Marshall, L. G., and Sempere, T., 1991, The Mesozoic and Paleocene vertebrates of Bolivia and their stratigraphic context: A review, *in* Suárez-Soruco, R., ed., Fósiles y facies de Bolivia, Vol. 1: Santa Cruz de la Sierra, Bolivia, Revista Técnica de YPFB (Yacimientos Petrolíferos Fiscales Bolivianos), v. 12, p. 393–433.

Gayet, M., Sempere, T., Cappetta, H., Jaillard, E., and Lévy, A., 1993, La présence de fossiles marins dans le Crétacé terminal des Andes centrales et ses conséquences paléogéographiques: Palaeogeography, Palaeoclimatology, Palaeoecology, v. 102, p. 28–319.

Gómez-Omil, R. J., Boll, A., and Hernández, R. M., 1989, Cuenca cretácico-terciaria del Noroeste argentino (Grupo Salta), *in* Chebli, G. A., and Spaletti, L. A., eds., Cuencas sedimentarias Argentinas: Serie correlación geológica: Tucumán, Argentina, Universidad Nacional de Tucumán, p. 43–64.

Haq, B. U., Hardenbol, J., and Vail, P. R., 1987, Chronology of fluctuating sea levels since the Triassic: Science, v. 35, p. 1156–1166.

Hérail, G., Oller, J., Baby, P., Sempere, T., Blanco, J., Bonhomme, M. G., and Soler, P., 1992, Las cuencas de Tupiza, Nazareno, Estarca: Sucesión de tectónica de transcurrencia y de cabalgamiento en la estructuración de los Andes de Bolivia: La Paz, X Congreso Geológico Boliviano, p. 81–83.

Jaillard, E., 1994, Kimmeridgian to Paleocene tectonic and geodynamic evolution of the Peruvian (and Ecuadorian) margin, *in* Salfity, J. A., ed., Cretaceous tectonics in the Andes: Earth evolution sciences monograph series: Wiesbaden, Germany, Vieweg, p. 101–167.

Jaillard, E., and Sempere, T., 1989, Cretaceous sequence stratigraphy of Peru and Bolivia: Simposios Sobre Cretácico de América Latina, Proceedings, p. A1–A27.

Jaillard, E., and Sempere, T., 1991, Las secuencias sedimentarias de la Formación Miraflores y su significado cronoestratigráfico: Santa Cruz de la Sierra, Bolivia, Revista Técnica de YPFB (Yacimientos Petrolíferos Fiscales Bolivianos), v. 12, p. 257–264.

Jaillard, E., Cappetta, H., Ellenberger, P., Feist, M., Grambast-Fessard, N., Lefranc, J. P., and Sigé, B., 1993, Sedimentology, paleontology, biostratigrahy and correlation of the Late Cretaceous Vilquechico Group of southern Peru: Cretaceous Research, v. 14, p. 623–661.

Jordan, T. E., and Alonso, R. N., 1987, Cenozoic stratigraphy and basin tectonics of the Andes mountains, 20°–28° South latitude: American Association of Petroleum Geologists Bulletin, v. 71, p. 49–64.

Kennan, L., 1993, Cenozoic evolution of the Cochabamba area, Bolivia: Oxford, United Kingdom, II International Symposium on Andean Geodynamics, p. 199–202.

Kennan, L., Lamb, S., and Rundle, C., 1995, K-Ar dates from the Altiplano and Cordillera Oriental of Bolivia: Implications for Cenozoic stratigraphy and tectonics: Journal of South American Earth Sciences, v. 8, p. 163–186.

Kennerley, J. B., 1980, Outline of the geology of Ecuador: London, United Kingdom, Institute of Geological Sciences, Overseas Geology and Mineral Resources, no. 55, 17 p.

Kirschvink, J. L., 1980, The least-squares line and plane and the analysis of palaeomagnetic data: Geophysical Journal of the Royal Astronomical Society, v. 62, p. 699–718.

Kley, J., 1993, Der Übergang vom Subandin zur Ostkordillere in Südbolivien (21°15′–22°S): Geologische Struktur und Kinematik: Berlin, Berliner Geowissenschaftliche Abhandlungen, Reihe A, v. 156, 88 p.

Leighton, M. W., and Kolata, D. R., 1991, Selected interior cratonic basins and their place in the scheme of global tectonics: A synthesis, *in* Leighton, M. W., Kolata, D. R., Oltz, D. F., and Eidel, J. J., eds., Interior cratonic basins: American Association of Petroleum Geologists Memoir, v. 51, p. 729–797.

Lohmann, H. H., and Branisa, L., 1962, Estratigrafía y paleontología del Grupo Puca en el synclinal de Miraflores, Potosí: La Paz, Petróleo Boliviano, v. 4, p. 9–16.

Marocco, R., Sempere, T., Cirbián, M., and Oller, J., 1987, Mise en évidence d'une déformation paléocène en Bolivie du Sud: Sa place dans l'évolution géodynamique des Andes centrales: Paris, Comptes Rendus de l'Académie des Sciences, sér. II, v. 304, p. 1139–1143.

Marshall, L. G., 1989, El primer diente de dinosaurio en Bolivia: Cochabamba, Bolivia, Revista Técnica de YPFB (Yacimientos Petrolíferos Fiscales Bolivianos), v. 10, p. 129–130.

Marshall, L. G., and Muizon, C. d., 1988, The dawn of the age of mammals in South America: National Geographic Research, v. 4, p. 23–55.

Marshall, L. G., and Sempere, T., 1991, The Eocene to Pleistocene vertebrates of Bolivia and their stratigraphic context: A review, *in* Suárez-Soruco, R., ed., Fósiles y facies de Bolivia, Vol. 1: Santa Cruz de la Sierra, Bolivia, Revista Técnica de YPFB (Yacimientos Petrolíferos Fiscales Bolivianos), v. 12, p. 631–652.

Marshall, L. G., Sempere, T., and Butler, R. F., 1997, Chronostratigraphy of the mammal-bearing Paleocene of South America: Journal of South American Earth Sciences (in press).

Mégard, F., 1989, The evolution of the Pacific Ocean margin in South America north of the Arica elbow (18°S), *in* Ben-Avraham, Z., ed., The evolution of the Pacific Ocean margins: Oxford, New York, Oxford University Press, p. 208–230.

Mourier, T., and 17 others, 1988, The Upper Cretaceous–lower Tertiary marine to continental transition in the Bagua basin, northern Peru: Paleontology, biostratigraphy, radiometry, correlations: Newsletters on Stratigraphy, v. 19, p. 143–177.

Muizon, C. d., 1991, La fauna de mamíferos de Tiupampa (Paleoceno inferior, Formación Santa Lucía), Bolivia, *in* Suárez-Soruco, R., ed., Fósiles y facies de Bolivia, Vol. 1: Santa Cruz de la Sierra, Bolivia, Revista Técnica de YPFB (Yacimientos Petrolíferos Fiscales Bolivianos), p. 575–624.

Odin, G. S., 1994, Geological time scale: Paris, Comptes Rendus de l'Académie des Sciences, sér. II, v. 318, p. 59–71.

Okamura, Y., and Mamani, B., 1994, Nannofósiles calcáreos de la Formación El Molino en el sinclinal de Miraflores, Departamento de Potosí: Revista Técnica de YPFB (Yacimientos Petrolíferos Fiscales Bolivianos), v. 15, p. 383–386.

Oller, J., and Sempere, T., 1990, A fluvio-eolian sequence of probable Middle Triassic–Jurassic age in both Andean and Subandean Bolivia: Grenoble, France, I International Symposium on Andean Geodynamics, p. 237–240.

Pardo-Casas, F., and Molnar, P., 1987, Relative motion of the Nazca (Farallon) and South American plates since Late Cretaceous time: Tectonics, v. 6, p. 233–248.

Pascual, R., Bond, M., and Vucetich, M. G., 1981, El subgrupo Santa Bárbara (grupo Salta) y sus vertebrados: Cronología, paleoambientes, y paleobiogeografía: San Luis, VIII Congreso Geológico Argentino, Proceedings, p. 743–758.

Pascual, R., Vucetich, M. G., and Fernández, J., 1978, Los primeros mamíferos (Notoungulata, Henricosbornidae) de la Formación Mealla (Grupo Salta, Subgrupo Santa Bárbara): Sus implicancias filogenéticas, taxonómicas y cronológicas: Ameghiniana, v. 15, p. 366–390.

Pérez, M., 1987, Datos palinológicos del Cretácico superior de la sección estratigráfica de Carata (Potosí, Bolivia): Santa Cruz de la Sierra, Bolivia, IV Congreso Latinoamericano de Paleontología, Proceedings, v. 2, p. 739–756.

Pilger, R. H., Jr., 1984, Cenozoic plate kinematics, subduction and magmatism: South American Andes: Journal of the Geological Society of London, v. 141, p. 793–802.

Ponce de León, V., 1966, Estudio geológico del sinclinal de Camargo: La Paz, Bolivia, Boletín del Instituto Boliviano del Petróleo, v. 6, p. 33–53.

Quattrocchio, M., 1978a, Contribución al conocimiento de la palinología estratigráfica de la Formación Lumbrera (Terciario inferior, Grupo Salta): Ameghiniana, v. 15, p. 285–300.

Quattrocchio, M., 1978b, Datos paleoecológicos y paleoclimatológicos de la Formación Lumbrera (Grupo Salta): Ameghiniana, v. 15, p. 173–182.

Quattrocchio, M. E., Marquillas, R. A., and Volkheimer, W., 1986, Palinología, paleoambientes y edad de la Formación Tunal, cuenca del Grupo Salta (Cretácico–Eoceno), República Argentina: Mendoza, IV Congreso Argentino de Paleontología y Bioestratigrafía, Proceedings, v. 3, p. 95–107.

Rage, J.-C., Marshall, L. G., and Gayet, M., 1993, Enigmatic Caudata (Amphibian) from the Upper Cretaceous of Gondwana: Geobios, v. 26, p. 515–519.

Ramos, V. A., 1988, The tectonics of the Central Andes; 30° to 33° S latitude, *in* Clark, S. P., Jr., Burchfiel, B. C., and Suppe, J., eds., Processes in continental lithospheric deformation: Geological Society of America Special Paper 218, p. 31–54.

Richards, D. R., 1995, Terranes and tectonic evolution of the Andes: A regional synthesis [Ph.D. dissert.]: Tucson, University of Arizona, 451 p.

Rouchy, J. M., Camoin, G., Casanova, J., and Deconinck, J. F., 1993, The central palaeo-Andean basin (Potosí area) during the Late Cretaceous and early Tertiary: Reconstruction of ancient saline lakes using sedimentological, palaeoecological, and stable isotope records: Palaeogeography, Palaeoclimatology, Palaeoecology, v. 105, p. 179–198.

Salfity, J. A., and Marquillas, R. A., 1981, Las unidades estratigráficas cretácicas del norte de la Argentina, *in* Volkheimer, W., and Musacchio, E. A., eds., Cuencas sedimentarias del Jurásico y Cretácico de América del Sur: Buenos Aires, Comité Sudamericano del Jurásico y Cretácico, p. 303–317.

Salfity, J. A., and Marquillas, R. A., 1994, Tectonic and sedimentary evolution of the Cretaceous–Eocene Salta Group Basin, Argentina, *in* Salfity, J. A., ed., Cretaceous tectonics in the Andes, Earth evolution sciences monograph series: Wiesbaden, Germany, Vieweg, p. 266–315.

Salinas, P., Sepúlveda, P., and Marshall, L. G., 1991, Hallazgo de restos óseos de dinosaurios (saurópodos) en la Formacion Pajonales (Cretácico superior), Sierra de Almeyda, II Región de Antofagasta, Chile: Implicancia cronológica: Viña del Mar, VI Congreso Geológico de Chile, p. 534–537.

Schamel, S., 1991, Middle and Upper Magdalena basins, Colombia, *in* Biddle, K. T., ed., Active

margin basins: World petroleum basin memoirs: Tulsa, Oklahoma, American Association of Petroleum Geologists, p. 283–301.
Sempere, T., 1990, Cuadros estratigráficos de Bolivia: Propuestas nuevas: Cochabamba, Revista Técnica de YPFB (Yacimientos Petrolíferos Fiscales Bolivianos), v. 11, p. 215–227.
Sempere, T., 1991, Cenozoic tectonic "phases" in Bolivia: Some needed clarifications: Viña del Mar, VI Congreso Geologico Chileno, v. 1, p. 877–881.
Sempere, T., 1992, The Cretaceous of Bolivia: A distal sedimentary record of the early central-Andean tectonic evolution: Salamanca, III Congreso Geológico de España y VIII Congreso Latino-Americano de Geología, Proceedings, v. 4, p. 80–84.
Sempere, T., 1994, Kimmeridgian? to Paleocene tectonic evolution of Bolivia, *in* Salfity, J. A., ed., Cretaceous tectonics of the Andes, Earth evolution sciences monograph series: Wiesbaden, Germany, Vieweg, p. 168–212.
Sempere, T., 1995, Phanerozoic evolution of Bolivia and adjacent regions, *in* Tankard, A. J., Suarez, R., and Welsink, H. J., eds., Petroleum basins of South America: American Association of Petroleum Geologists Memoir 62, p. 207–230.
Sempere, T., Oller, J., Cherroni, C., Araníbar, O., Barrios, L., Cirbián, M., and Pérez, M., 1987, Un ejemplo de cuenca carbonatada en un contexto distensivo de retroarco: Paleogeodinámica del Cretácico terminal en le República de Bolivia (Formación El Molino y equivalentes): Tucumán, X Congreso Geológico Argentino, Abstracts, v. PICG 242, p. 18–19.
Sempere, T., Oller, J., and Barrios, L., 1988, Evolución tectosedimentaria de Bolivia durante el Cretácico: Santiago de Chile, V Congreso Geológico Chileno, Proceedings, v. 3, p. H37–H65.
Sempere, T., Baby, P., and Oller, J., 1989, Geologic structure and tectonic history of Bolivian orocline: International Geological Congress, 28th, Washington, D.C., Abstracts, p. 3-72–3-73.
Sempere, T., Hérail, G., Oller, J., and Bonhomme, M. G., 1990, Late Oligocene–early Miocene major tectonic crisis and related basins in Bolivia: Geology, v. 18, p. 946–949.
Sempere, T., Baby, P., Oller, J., and Hérail, G., 1991, La nappe de Calazaya: Une preuve de raccourcissements majeurs gouvernés par des éléments paléostructuraux dans les Andes boliviennes: Paris, Comptes Rendus de l'Académie des Sciences, sér. II, v. 312, p. 77–83.
Soler, P., and Bonhomme, M. G., 1990, Relation of magmatic activity to plate dynamics in central Peru from Late Cretaceous to present, *in* Kay, S. M., and Rapela, C., eds., Plutonism from Antarctica to Alaska: Geological Society of America Special Paper 241, p. 171–192.
Soler, P., Carlier, G., and Marocco, R., 1989, Evidence for subduction and underplating of an oceanic plateau beneath the south Peruvian margin during the Late Cretaceous: Structural implications: Tectonophysics, v. 163, p. 13–24.
Vergani, G. D., Tankard, A. J., Belotti, H. J., and Welsink, H. J., 1995, Tectonic evolution and paleogeography of the Neuquén basin, Argentina, *in* Tankard, A. J., Suárez R. S., and Welsink, H. J., eds., Petroleum basins of South America: American Association of Petroleum Geologists Memoir 62, p. 383–402.
Volkheimer, W., Quattrocchio, M., and Salfity, J., 1984, Datos palinológicos de la Formación Maíz Gordo, Terciario inferior de la cuenca de Salta: San Carlos de Bariloche, IX Congreso Geológico Argentino, Proceedings, v. 4, p. 523–538.
Watson, G. S., 1956, A test for randomness of directions: Monthly Notices, Geophysical Journal of the Royal Astronomical Society, v. 7, p. 160–161.
Wignall, P. B., 1991, Model for transgressive black shales?: Geology, v. 19, p. 167–170.
Wilson, T. J., 1991, Transition from back-arc to foreland basin development in the southernmost Andes: Stratigraphic record from the Ultima Esperanza District, Chile: Geological Society of America Bulletin, v. 103, p. 98–111.
Winslow, M. A., 1982, The structural evolution of the Magallanes basin and neotectonics in the southernmost Andes, *in* Craddock, C., ed., Antarctic geoscience: Madison, University of Wisconsin Press, p. 143–154.

MANUSCRIPT RECEIVED BY THE SOCIETY FEBRUARY 13, 1996
REVISED MANUSCRIPT RECEIVED SEPTEMBER 25, 1996
MANUSCRIPT ACCEPTED OCTOBER 19, 1996

Printed in U.S.A.